Electronic *versus* steric control in palladium complexes of carboranyl phosphine-iminophosphorane ligands[i]

José Luis Rodríguez-Rey[a], David Esteban-Gómez[b], Carlos Platas-Iglesias[b] and Antonio Sousa-Pedrares[a*]

[a] Departamento de Química Inorgánica, Universidade de Santiago de Compostela, 15782 Santiago de Compostela, Spain

[b] Centro de Investigacións Científicas Avanzadas (CICA) and Departamento de Química, Universidade da Coruña, Campus da Zapateira-Rúa da Fraga 10, 15008 A Coruña, Spain

Dalton Transactions, volume 48, issue 2, pages 486–503, 14 January 2019
Submitted 5 October 2018, accepted 29 November 2018, first published 30 November 2018

How to cite:

J. L. Rodríguez-Rey, D. Esteban-Gómez, C. Platas-Iglesias and A. Sousa-Pedrares, Electronic versus steric control in palladium complexes of carboranyl phosphine-iminophosphorane ligands, *Dalt. Trans.*, 2019, **48**, 486–503. DOI: 10.1039/C8DT04006K.

Abstract

A new family of carboranyl phosphine-iminophosphorane ligands was prepared and characterized. The new ligands present a carboranyl group directly attached to the iminophosphorane nitrogen atom through a cage carbon atom (C-carboranyl derivatives **L1–L3**) or through the B3 boron atom (B-carboranyl derivatives **L4** and **L5**), and the phosphine group on a side chain derived from the diphosphine *dppm*, *i.e.* with a two-atom spacer between the P and N donor atoms. The non-carboranyl analogue **L6**, with a biphenyl group on the nitrogen atom, was also synthesized for comparison. These potential (P, N) ligands were used to obtain palladium complexes (**Pd1–Pd6**) and, thus, study how the different inductive effect of the carboranyl substituents can modify the coordinating ability of the nitrogen atom. The structural analysis of the complexes revealed two different coordination modes for the ligands: the (P, N) chelate coordination and the unexpected P-terminal coordination, which is not observed for non-carboranyl phosphine-iminophosphoranes. These unexpected structural differences led us to perform DFT calculations on the ligands and metal complexes. The calculations show that the final coordination modes depend on the balance between the electronic and steric properties of the particular carboranyl group.

Introduction

ortho-Carboranes are bulky clusters with ten boron atoms and two adjacent carbon atoms in an icosahedral arrangement. The B–H hydride bonds confers them a high hydrophobic character, while the close shell structure gives them high thermal and chemical stability.[1] The functionalization of other materials with carborane substituents has been used to produce robust materials[2] and hydrophobic compounds that have found several medical applications.[3] The carborane molecule is a bulky cluster, comparable to adamantane and significantly larger than the phenyl ring rotation envelope.[4] Thus, it has found application as a steric group, for example for the construction of luminescent materials, as the bulky cage can hinder intermolecular

* antonio.sousa.pedrares@usc.es

interactions.[5] A very interesting property of the *o*-carborane cluster is its irregular charge distribution. It has been established that the CH vertices, with more electron density involved in the skeletal electrons are holders of $+\delta$ charges, and that the electron density on the BH vertices increases with the distance from the CH vertices, increasing the $-\delta$ charge on the boron atoms.[6] Thus, the electron density of the five different positions of the *ortho*-carborane moiety (Fig. 1), follow the order: 1 (2) < 3 (6) < 4 (5, 7, 11) < 8 (10) < 9 (12) (1, 2: carbon atoms; 3–12: boron atoms). This order of electron density is reflected in the inductive effect that every position of the cluster exerts on its hydrogen atom or on any group that may substitute it. Thus, the cluster carbon atoms show a clear electron-withdrawing character, which is less pronounced for the B3/B6 positions (connected to both carbon atoms). The boron atoms at the central positions (B4, B5, B7, B11) are electroneutral, while the further boron atoms B8/B10, and especially the antipodal positions B9/B12, are electron-donating. These irregularities determine the reactivity of every position and, thus, the possibility of preparing substituted derivatives. The electron-withdrawing character of the carbon atoms is reflected in acidic CH groups (pK_a = 23.3),[7] which is commonly exploited for the preparation of C-functionalized carboranes (*via* deprotonation with strong bases and reaction with electrophiles).[1] The positively charged boron atoms, B3 and B6, react with nucleophiles to produce *nido* derivatives,[8] which can be capped to yield *closo*-B3-functionalized derivatives.[1,9] The electron-donating character of the antipodal B9/B12 positions is reflected in a higher reactivity towards electrophilic substitution (which proceeds to the B8 and B10 positions under forcing conditions), which enables the easy preparation of other B-functionalized carboranes.[1]

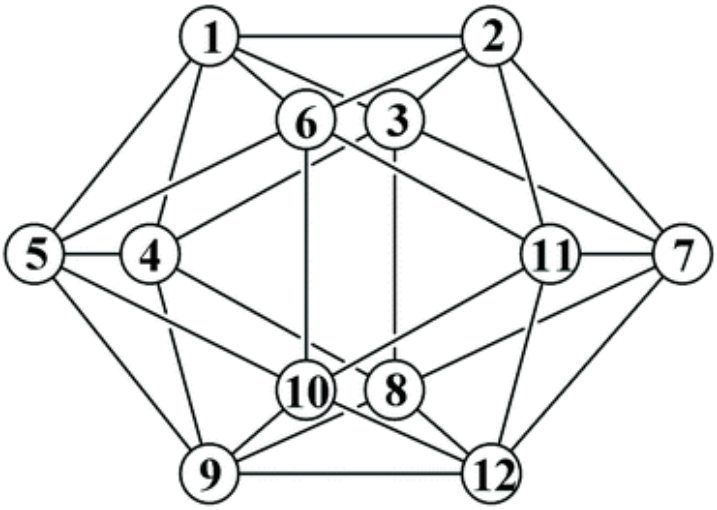

Fig. 1. Numbering scheme used for *o*-carborane derivatives (1,2: carbon atoms; 3–12: boron atoms). Equivalent positions: (C1, C2), (B3, B6), (B4, B5, B7, B11), (B8, B9), (B9, B12).

The different inductive effect of C- and B-carboranyl derivatives has been used to modify chemical and physical properties of other substrates. However, most of these studies only exploit the electron-withdrawing character of C-carboranyl derivatives. In fact, this character leads to unique electronic effects and has been used for the preparation of electronic and luminescent materials.[5] The few studies that compare the different inductive effect of C- and B-carboranyl groups have only focused on the more extreme members of the series, *i.e.* the electron-withdrawing C-carboranyl derivatives and the electron-donating B8- and B9-carboranyl derivatives. Thus, carboranyl groups have been used to modify the acidity of carboxylic acid[6b] and thiol groups (–SH),[6c,d] concluding, for example, that the C-connection increases the acidity of a –SH group (pK_a = 3.30) while the B8- (pK_a = 9.32) and B9- (pK_a = 10.08) connections decrease the acidity, compared to a phenyl ring (pK_a = 7.50).[6c,d] In the field of coordination chemistry, the carboranyl group has

also been used to modify the coordinating strength of vicinal donor atoms. Once again, these studies have only taken into account the deactivating C-carboranyl moiety and the donating B9-carboranyl group. Published results report the reduction of the coordinating strength of C-carboranyl phosphines[10] and thioethers,[11] and the enhancement of the strength for B9-thioethers.[11] Some of us have also contributed to this field by studying the deactivation of the coordinating ability of an iminophosphorane nitrogen donor atom by effect of a C-carboranyl group.[12,13] Iminophosphoranes, $R_3P = NR'$, are basic compounds that can act as ligands though the sp^2-hybridized nitrogen atom of their highly polarized P═N bond. They are predominantly σ-donor ligands with no significant π-accepting capacity. Although the basicity of the nitrogen atom depends on its substituent (R′),[14] neutral iminophosphoranes can be usually exchanged by other ligands.[15] However, the combination with stronger donors produces more stabilizing chelating ligands that enable the preparation of stable coordination complexes, some of them with interesting catalytic activities.[15,16] Our recent studies on carboranyl-iminophosphoranes increased the limited knowledge on these compounds,[17,18] and showed that the nitrogen donor atom is very affected by the C-carboranyl group, although its donating properties are also influenced by the nature of the second (more coordinating) donor atom on the other cage carbon atom.

The combination with a thiolate group (Fig. 2, $E = S^-$) completely deactivates the nitrogen atom towards the coordination to a palladium(ii) center,[12] while the combination with a phosphine group (Fig. 2, $E = PPh_2$) reduces its coordination strength although the ligand can still engage in (P, N) coordination to a palladium center.[13] However, while the phosphine group was proven to favor the coordination of the nitrogen atom, the direct connection of both neutral donor groups (phosphine and iminophosphorane) to the cage carbon atoms promotes the evolution to the anionic *nido* derivatives which results in an increase of the donor strength of the nitrogen atom,[13] as also found for 10 and 12-vertex *closo*-carborane anions, which are strong electron donor substituents.[19]

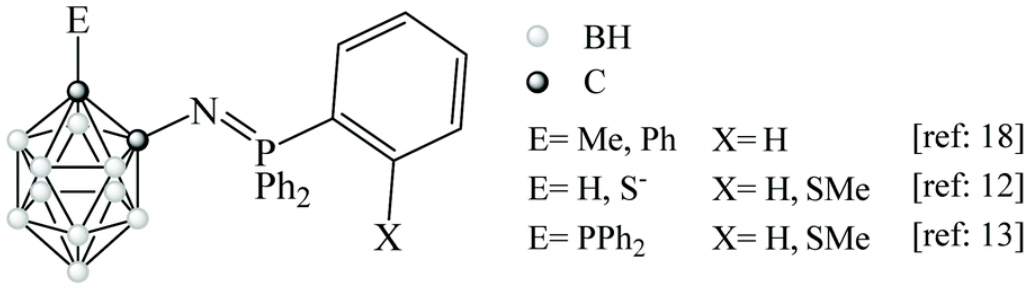

Fig. 2. *closo*-Carboranyl-iminophosphoranes reported in the literature.

As a continuation of our research on the modulation of the coordinating ability of an iminophosphorane nitrogen atom by effect of a carborane group, we have designed new carboranyl phosphine-iminophosphorane ligands with the nitrogen atom directly attached to a cage atom (C- or B3-), and the more coordinating phosphine group on a side chain, to favor N-coordination by chelate effect but without promoting the evolution to *nido* derivatives (Fig. 3). Although no studies have been reported so far on the inductive effect of B3-carboranes, we have chosen the C- and B3-points of attachment to the carborane cage as they are both associated with electron-withdrawing character, although to a different extent. Thus, these ligands allow us to compare the different deactivating modifications that the carborane cage can induce on the nitrogen donor atom, and provide valuable information regarding the design principles associated with the phosphine-iminophosphorane ligand system.

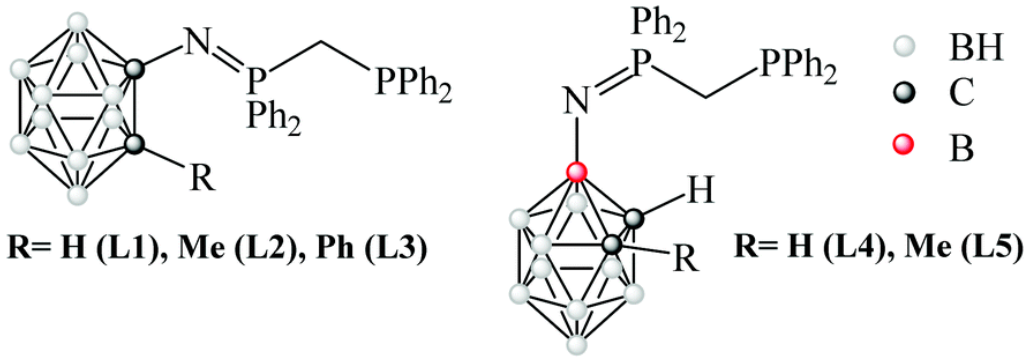

Fig. 3. Carboranyl phosphine-iminophosphorane ligands (**L1–L5**) designed for this study.

Results and discussion

Synthesis and characterization of the carborane ligands

The designed carboranyl phosphine-iminophosphorane ligands (**L1–L5**, Fig. 3) were obtained following the Staudinger method,[20] *i.e.* by reaction of B- or C-carboranyl-azides and 1,1-bis(diphenylphosphino)methane (*dppm*). The difference between the synthesis of C-carboranyl and B-carboranyl iminophosphoranes lies in the different method for the *in situ* preparation of the corresponding carboranyl-azide. In the case of the C-carboranyl derivatives (ligands **L1–L3**), the preparations of the R-carboranyl-azides have been described in the literature, R = H,[12] Me,[18,21] Ph.[18] The reaction of the different C-carboranyl azides, obtained *in situ*, with the equimolar amount of the diphosphine *dppm*, yields the projected C-carboranyl phosphine-iminophosphoranes **L1–L3** (Scheme 1). This method has already been reported for the preparation of the other known *closo*-C-carboranyl iminophosphoranes (Fig. 2).[12,13,18]

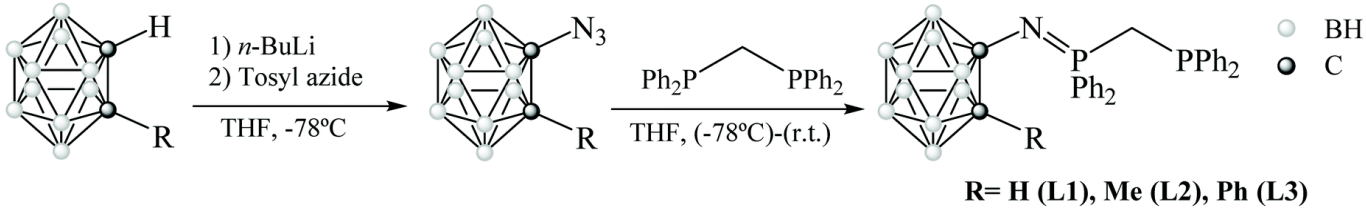

Scheme 1. Synthesis of the C-carboranyl phosphine-iminophosphoranes **L1–L3**.

In the case of the B-carboranyl derivatives (ligands **L4** and **L5**, Scheme 2), although the synthesis of 3-azide-carborane has been described in the literature using 3-diazonium-*o*-carborane tetrafluoroborate as starting material,[22] we decided to apply the method described for the preparation of organic aromatic azides, starting from the corresponding amines.[23] Thus, this method requires the previous synthesis of the different 3-amine-carborane precursors (R = H, Me, Scheme 2), which are described in the literature.[24,25] The versatile 1-R-3-NH_2-*o*-caborane derivatives have been previously used as precursors of other nitrogen functionalities, like amines,[26] isocyanes,[27] and diazonium salts,[22] which, in turn, have been used to prepare other B3-substituted carboranes.[22,28] However, they have never been used to prepare 3-azide derivatives. The isolated B-carboranyl amines (Scheme 2) were converted into the desired azides under mild conditions, by reaction with *tert*-butyl nitrite and azidotrimethylsilane.[23] The azides, obtained *in situ*, were reacted with one equivalent of diphosphine *dppm*, yielding the projected B-carboranyl phosphine-iminophosphoranes **L4** and **L5** (Scheme 2).

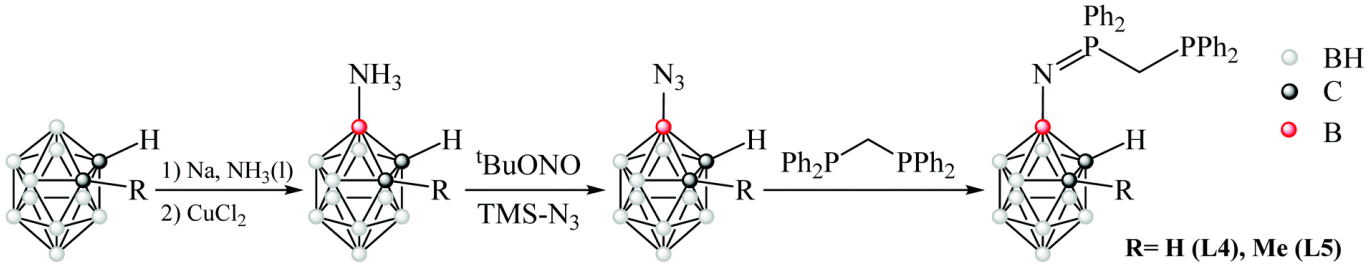

Scheme 2. Synthesis of the B-carboranyl phosphine-iminophosphoranes **L4** and **L5**.

Due to the few number of palladium complexes with phosphine-iminophosphorane ligands described in the literature (see below), we decided to synthesize the non-carboranyl phosphine-iminophosphorane analogue **L6**, with a bulky biphenyl substituent on the iminophosphorane nitrogen atom, which provides a good comparison with the carboranyl ligands. Ligand **L6** was obtained following the same procedure used for the B-carboranyl derivatives, *i.e.* by reaction of diphosphine dppm with 1-azido-2-phenylbenzene, obtained *in situ* from 2-phenyl-aniline (Scheme 3).[23]

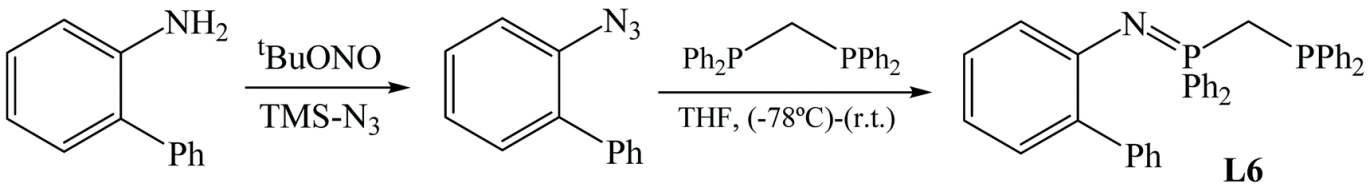

Scheme 3. Synthesis of the organic phosphine-iminophosphorane **L6**.

The analysis of solid samples of the carboranyl ligands **L1–L5** by IR spectroscopy confirms the presence of the *closo*-carborane cage, as the spectra exhibit a very intense *ν*(B–H) band in the range 2566–2588 cm^{-1}, typical of *closo*-carborane derivatives. The IR spectra of **L1–L6** also show an intense band attributable to the *ν*(P═N) stretching frequency (1304–1433 cm^{-1}) that proves the formation of the iminophosphorane P═N bond (Table 1). These values are similar to those found for other free carboranyl-iminophosphorane derivatives described in the literature (Fig. 2), in the range 1332–1423 cm^{-1},[12,13,18] and also similar to those found for non-coordinated (non-carboranyl) aromatic derivatives.[29] A detailed analysis of the data shows the different strength of the P═N bond depending on the type of ligands, which is reflected in different ranges for the C-carboranyl ligands **L1–L3**, 1304–1375 cm^{-1}, and the B-carboranyl ligands **L4** (1433 cm^{-1}) and **L5** (1374 cm^{-1}) more similar to the organic ligand **L6** (1429 cm^{-1}).

The ^{31}P spectra of all of **L1–L6** consist of two doublets (see Table 1). The signal observed at higher field was assigned to the P(iii) phosphine group (–PPh_2) and the other one to the P(v) iminophosphorane group (P═N). The chemical shift of the signal due to the phosphine group (–PPh_2) does not depend on the nature of the substituent on the nitrogen atom (carboranyl or non-carboranyl), as **L6** shows this signal at −29.6 ppm, while for the carboranyl ligands **L1–L5** they are observed in the range (−30.9)–(−29.9) ppm. Other unbound phosphine-iminophosphorane ligands derived from the diphosphine *dppm* found in the literature also show very similar values for the –PPh_2 group, near −29 ppm.[30–33] However, the signal due to the P(v) iminophosphorane group (P═N) is sensitive to the nature of the group on the nitrogen atom. Thus, the carboranyl ligands **L1–L5** show these signals in the range 5.8–9.1 ppm, while the signal found for the iminophosphorane group in the spectrum of **L6** (−1.2 ppm) is shifted to higher field with respect to the carboranyl ligands. The deshielding of the iminophosphorane phosphorus atom by effect of the carboranyl

cage reflects its electron-withdrawing character. Other unbound phosphine-iminophosphorane ligands derived from the diphosphine *dppm* found in the literature also show different values for the P═N–R group depending on the electron-withdrawing character of the R group on the nitrogen atom. Thus, *N*-aryl (organic) derivatives show values for the iminophosphorane phosphorus atom at highfield, between 0 and 5 ppm,[31–33] while derivatives with electron-withdrawing groups on the nitrogen atom show the signals of the P(v) phosphorus atom shifted to lower fields (10–12 ppm, R = phenyl rings with –F, –CN or $–NO_2$ substituents).[34,35] The latter values, shifted to low field, are more similar to those found for the carboranyl ligands **L1–L5**. However, it is interesting to note that the pairs of C- and B-carboranyl analogues show almost the same chemical shifts for the P(v) atom (5.9 and 5.8 for **L1** and **L4**, respectively, and 9.1 and 8.1 ppm for **L2** and **L5**, respectively), which does not reflect the more electron-withdrawing character of the C-carboranyl derivatives compared to the B-carboranyl ones.

Table 1. Selected spectroscopic data (IR and ^{31}P NMR) for ligands **L1–L6**.

	IR	^{31}P NMR[a]		
	ν(PN)/cm^{-1}	$–PPh_2$	P═N	$^2J_{P,P}$
L1	1370	−30.9	5.9	54.7
L2	1304	−30.1	9.1	57.0
L3	1375	−30.5	7.4	56.6
L4	1433	−30.2	5.8	50.8
L5	1374	−29.9	8.1	52.7
L6	1429	−29.6	−1.2	52.0

[a] Chemical shifts in ppm and coupling constants in Hz.

The ^{1}H NMR spectra of the ligands show signals due to the diphosphine fragment and to the groups on the nitrogen atom; the carborane cage (**L1–L5**) or the biphenyl group (**L6**). The more interesting signals of the diphosphine fragment are those due to the aliphatic protons of the methylene spacer, which appear as one multiplet in the range 2.89–3.32 ppm, due to coupling with both phosphorus atoms. The organic ligand **L6** presents a very similar chemical shift for these protons (3.27 ppm). The ^{1}H NMR spectra of the carboranyl ligands also show signals due to the carborane cage. Except in the cases of the disubstituted C-carboranyl ligands (**L2** and **L3**) the spectra show signals due to the protons on the cage carbon atoms (Cc–H). The C-carboranyl derivative **L1** shows this signal at 3.69 ppm, slightly deshielded compared to the B-carboranyl analog **L4**, 3.03 ppm. The substitution of one of the cage carbon atoms of the B-carboranyl derivative with a methyl group further shifts the Cc–H signal to high field (δ = 2.69 ppm for **L5**). The methyl group of the C-carboranyl ligand **L2** (2.01 ppm) appears only slightly downfield shifted with respect to the B-carboranyl ligand **L5** (1.90 ppm). These chemical shifts are very similar to those reported for 1-triphenyliminophosphorane-2-methyl-carborane (2.02 ppm).[23]

The ^{11}B NMR spectra show very similar ranges for the C-carboranyl derivatives (**L1–L3**), with signals between −15.7 and −5.9 ppm, typical of *closo*-carborane compounds. The B-carboranyl derivatives, **L4** and **L5**, show signals in wider ranges, (−23.3)–(2.0) ppm, with the resonance due to the substituted boron atom at lower field. This signal, which is the only one with a positive shift, is very easy to assign by comparing the ^{1}H decoupled ^{11}B NMR spectrum with the coupled one, as this is the only boron atom not attached to a hydrogen atom (see spectra in ESI[i]). The ranges of signals shown by the B-carboranyl iminophosphoranes are also wider than those found for other nitrogen-substituted B-carboranyl compounds found in the

literature, like 3-amino-carborane [(−19.14)–(0.14) ppm],[28] 3-nitro-carborane [(−14.8)–(−3.5) ppm],[26] 3-azido-carborane [(−14.2)–(−3.8) ppm],[26] 3-amide derivatives [(−15)–(−3) ppm, aprox.],[22,24,36a] 3-triazol derivatives [(−12.9)–(−2.8) ppm],[36b] or 3-amine derivatives [(−17)–(−1) ppm, aprox.].[22,36c] It is interesting to note that none of the literature examples present positive shifts for the substituted boron atom, indicating a more deshielding effect for the iminophosphorane substituent.

Synthesis and characterization of the palladium complexes

The neutral carboranyl phosphine-iminophosphorane ligands **L1–L5**, which are potentially (P, N) bidentate ligands, were used to synthesize palladium complexes and thus compare their coordinating abilities. The ligands were stirred overnight with the palladium precursor *cis*-$[PdCl_2(PhCN)_2]$[37] in a 1 : 1 molar ratio in dry tetrahydrofuran at room temperature (see Schemes 4 and 5). The substitution of the labile benzonitrile ligands of the precursor leads to the formation of new palladium complexes, which were precipitated from the solution by adding hexane (see Experimental section). The organic ligand **L6** was also used to prepare a similar palladium complex under the same conditions, **Pd6** (see Scheme 6).

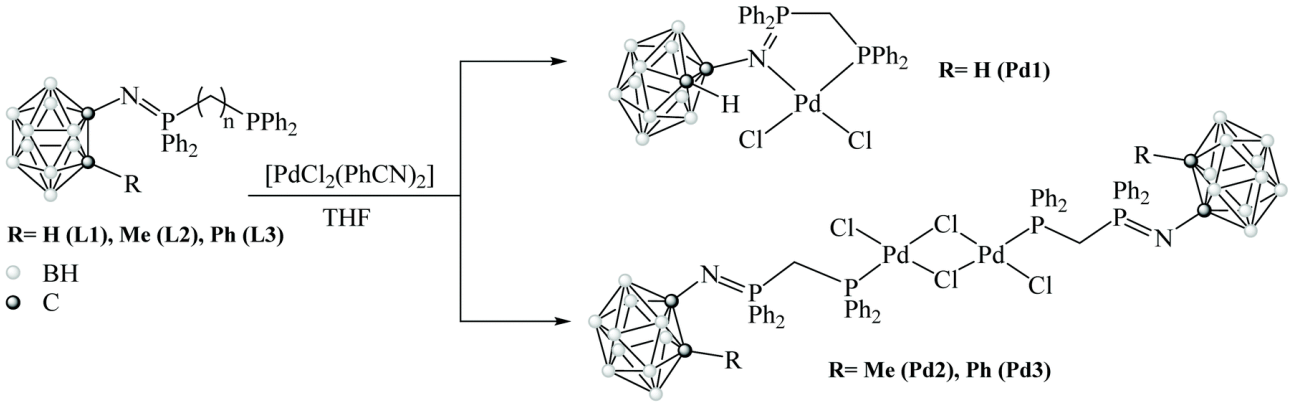

Scheme 4. Synthesis of palladium complexes with C-carboranyl phosphine-iminophosphorane ligands, **Pd1–Pd3**.

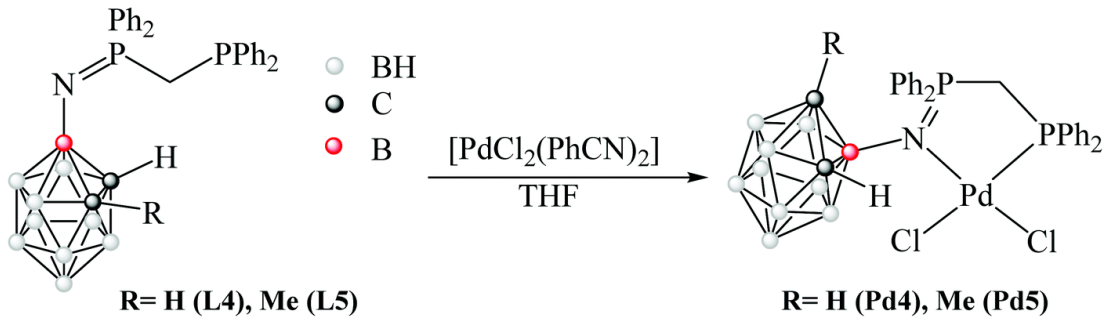

Scheme 5. Synthesis of palladium complexes with B-carboranyl phosphine-iminophosphorane ligands, **Pd4** and **Pd5**.

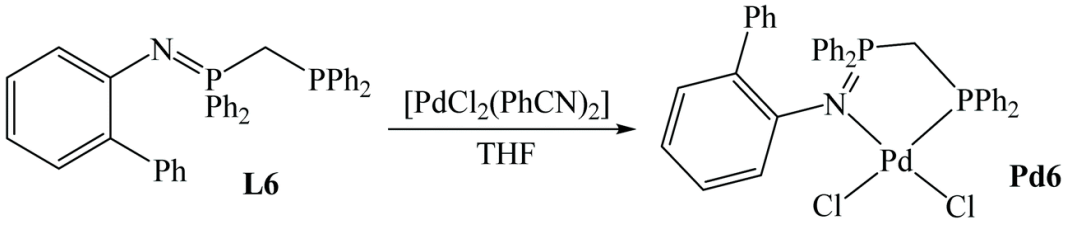

Scheme 6. Synthesis of the palladium complex with the organic phosphine-iminophosphorane ligand, **Pd6**.

All the palladium complexes **Pd1**–**Pd6** were characterized by standard spectroscopic techniques, elemental analysis and X-ray diffraction analysis. Although the spectroscopic techniques evidence the presence of the ligands in the complexes, the X-ray studies were crucial to assign the coordination modes of the phosphine-iminophosphorane ligands. The X-ray studies (see below) revealed two different coordination modes for these ligands: P-terminal ligands (dimeric complexes **Pd2** and **Pd3**, see Scheme 4) and (P, N) chelating ligands (monomeric complexes **Pd1**, **Pd4**–**6** see Schemes 4–6).

The IR spectra of the palladium complexes are very informative. The integrity of the *closo*-carborane cage is reflected in the values of the strong ν(B–H) bands, 2551–2587 cm^{-1}, which show almost the same range as the free *closo*-carboranyl ligands (see before). However, the most interesting band of the IR spectra of the metal complexes is the strong band associated with the iminophosphorane stretching frequency, ν(P═N) (see Table 2). This band is sensitive to the coordination of the iminophosphorane group to a metal atom, which weakens the P–N bond and thus, shifts the band to lower wavenumbers.[38] The extent of the shift can be used to estimate the strength of the metal–ligand interaction. The palladium complexes **Pd2** (1336 cm^{-1}) and **Pd3** (1396 cm^{-1}) with disubstituted C-carboranyl ligands, show ν(P═N) bands at almost the same values as the corresponding free ligands. These bands are even shifted to higher wavenumbers (positive shifts of 32 and 21 cm^{-1}, respectively), which indicates that the iminophosphorane nitrogen atom is not coordinated to the palladium atom in these cases. This result is in accordance with the P-terminal coordination mode revealed for these complexes by X-ray crystallography. For the rest of the palladium complexes, with ligands with (P, N) chelating mode, the ν(PN) bands are shifted to lower wavenumbers respect to the corresponding bands of the free ligands, due to the formation of the Pd–N bond. However, there is a difference between the shift found for the C-carbonyl derivative **Pd1**, ($\Delta\nu$ = −132 cm^{-1}), and those found for the B-carboranyl derivatives **Pd4** ($\Delta\nu$ = −180 cm^{-1}) and **Pd5** ($\Delta\nu$ = −152 cm^{-1}), more similar to the shift found for the non-carboranyl complex **Pd6** ($\Delta\nu$ = −158 cm^{-1}).

Table 2. Selected spectroscopic data (IR and ^{31}P NMR) for the palladium complexes **Pd1**–**Pd6**[a].

		IR/cm^{-1}		^{31}P NMR[b]					
	Coord. Mode	ν(PN)	Δ(PN)	–PPh_2	$\Delta\delta$	P═N	$\Delta\delta$	$^2J_{P,P}$	$\Delta(^2J_{P,P})$
Pd1	(P,N)-Chelate	1238	−132	8.2	39.1	38.2	32.3	32.7	−22
Pd2	P-Terminal	1336	32	20.5	50.6	17.5	8.4	8.6	−48.4
Pd3	P-Terminal	1396	21	20.6	51.1	2.1	5.3	13.9	−42.7
Pd4	(P,N)-Chelate	1253	−180	11.4	41.6	40.9	35.1	27.6	−23.2
Pd5	(P,N)-Chelate	1222	−152	9.6	39.5	40.8	32.7	28.4	−24.3
Pd6	(P,N)-Chelate	1271	−158	12.9	42.5	41.7	42.9	35.2	−16.8

[a] Δ values are the differences with respect to the corresponding free ligands. [b] Chemical shifts in ppm and coupling constants in Hz.

The palladium complexes were also characterized by NMR spectroscopy (^{31}P, ^{1}H and ^{11}B). The ^{31}P NMR spectra of the palladium complexes show two doublets due to the coupling of the two phosphorus groups, phosphine (–PH_2) and iminophosphorane (PN) (see data in Table 2). However, the assignment of the peaks is not straightforward, as it depends on the coordination mode of the ligand. The assignment was possible due to the knowledge of the coordination mode of the ligands in the complexes (provided by X-ray crystallography) and by comparison with literature data for other palladium complexes with similar organic ligands. The dimeric palladium complexes **Pd2** and **Pd3**, $[PdCl_2(L)]_2$, present P-terminal disubstituted C-carboranyl ligands (Scheme 4). The signal due to the phosphine group is not affected by the different substitution of the carborane cage, being observed at 20.5 ppm for **Pd2** and 20.6 ppm for **Pd3**. These signals are shifted downfield to ∼50 ppm respect to the signals of the free ligands, which confirms the formation of the Pd–P bond. While metal complexes with P-terminal organic phosphine-iminophosphorane ligands are not reported in, the literature, examples of similar palladium dimers with terminal phosphines show one singlet signal in the ^{31}P NMR spectra, usually between 25 and 40 ppm, that experiences important shifts with respect to the free ligands.[39,40] The other signal in the ^{31}P NMR spectra of the dimeric complexes **Pd2** (17.5 ppm) and **Pd3** (2.1 ppm) can be assigned to the iminophosphorane phosphorus atom. These signals at high field are not very shifted respect to the corresponding signals of the free ligands (see Table 2), which is in agreement with the P-terminal coordination found for the ligands in the solid state. The rest of the synthesized palladium complexes (**Pd1**, **Pd4**–**Pd6**) present phosphine-iminophosphorane ligands with (P, N) coordination, as shown by X-ray crystallography. The literature reports several examples of palladium complexes with non-carboranyl phosphine-iminophosphorane ligands, all of them with (P, N) chelating coordination. By comparison with literature data,[30–34,41,42] the assignment of the ^{31}P NMR spectra of these complexes was reversed compared to the complexes with P-terminal ligands, *i.e.* the signal at high field (8.2–12.9 ppm) was assigned to the –PPh_2 group and the signal at low field (38.2–41.7 ppm) was assigned to the PN group (see Table 2). In all cases, both signals are very shifted downfield with respect to the signals of the free ligands by effect of the (P, N) coordination, although for each complex this effect is more pronounced for the phosphine group than for the PN group (Table 2), as also found for the literature examples.[35a] For these cases with (P, N) coordination, the magnitude of the $^{2}J_{PP}$ coupling constants decreases upon complexation ($\Delta \approx -20$ Hz), as shown in Table 2. In conclusion, although the ^{31}P data is in agreement with the structures found in the solid state by X-ray crystallography, the similarities among the spectra of the different complexes, regardless the coordination mode of the ligand, make difficult the assignment of the signals without the previous knowledge of the final structures.

The ^{1}H NMR spectra of the palladium complexes show the same signals as the corresponding free ligands, proving the presence of the ligands in the complexes. The signal due to the Cc–H group of complexes **Pd1** (5.15 ppm) **Pd4** (5.16 ppm) and **Pd5** (6.05 ppm) appears shifted to lower field compared to the free ligands. The extent of the shift observed upon ligand coordination appears to reflect the strength of the Pd–N interaction, as it is lower for the complex with the more withdrawing C-carboranyl ligand, **Pd1** (Δ = 1.43 ppm), than for the complexes with B-carboranyl ligands, **Pd4** (Δ = 2.13 ppm) and **Pd5** (Δ = 3.36 ppm). The ^{1}H NMR spectra of the palladium complexes also show the signals due to the aliphatic protons of the methylene spacer. These signals are slightly shifted compared to the corresponding signals of the free ligands, but to a different extent depending on the particular case, without a clear influence of the coordination mode of the ligand. The spectra of the complexes **Pd2** and **Pd5** also show the singlet signal due to methyl group at higher field (1.27 and 2.11 ppm respectively).

The ^{11}B NMR spectra of the palladium complexes with carboranyl ligands show broad resonances in the range (−0.4)–(−17.9) ppm, confirming the presence of the *closo*-carborane cage. The complexes with B-carboranyl ligands [(−0.4)–(−17.9) ppm] show wider ranges than the complexes with C-carboranyl ligands [(−3.9)–(−17.1) ppm], although to a lesser extent than the free ligands (see before). The spectra of the B-carboranyl derivatives **Pd4** and **Pd5**, show the signal due to the B3 boron atom at higher field (−0.4 and −1.2

ppm, respectively) than the corresponding free ligand (1.4 ppm for **L4** and 2.0 ppm for **L5**), by effect of the Pd–N coordination.

Crystal structures of the metal complexes Pd1–Pd6

Single crystals suitable for X-ray diffraction analysis of all the palladium complexes were obtained by slow concentration of solutions of the complexes in mixtures of dichloromethane and hexane, except in the case of **Pd6**, that was recrystallized from a mixture of chloroform and hexane. The molecular structures of the complexes are shown in Fig. 4–9. The crystallographic data can be found in Table S1 (ESI[i]). Selected bond lengths and angles for these compounds are collected in Tables 3–5.

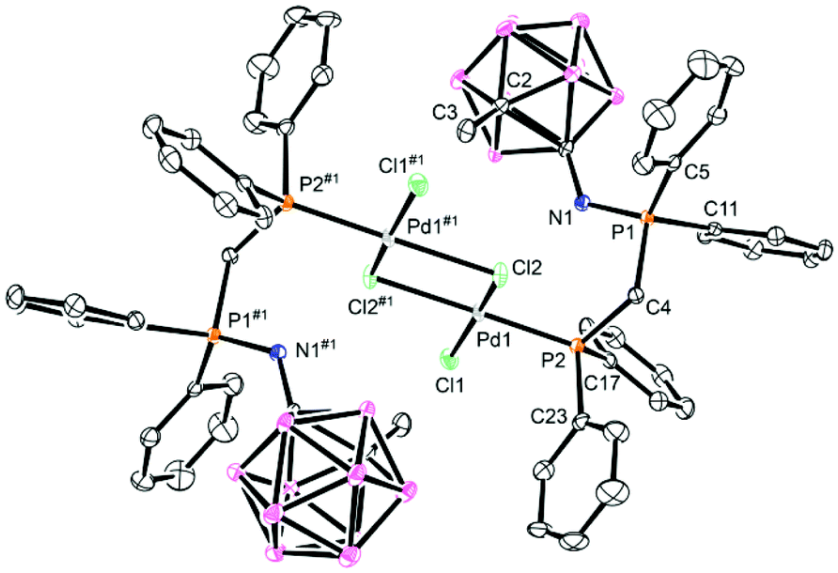

Fig. 4. Molecular structure of compound **Pd2**. Thermal ellipsoids are shown at the 40% probability level. Hydrogen atoms are omitted for clarity.

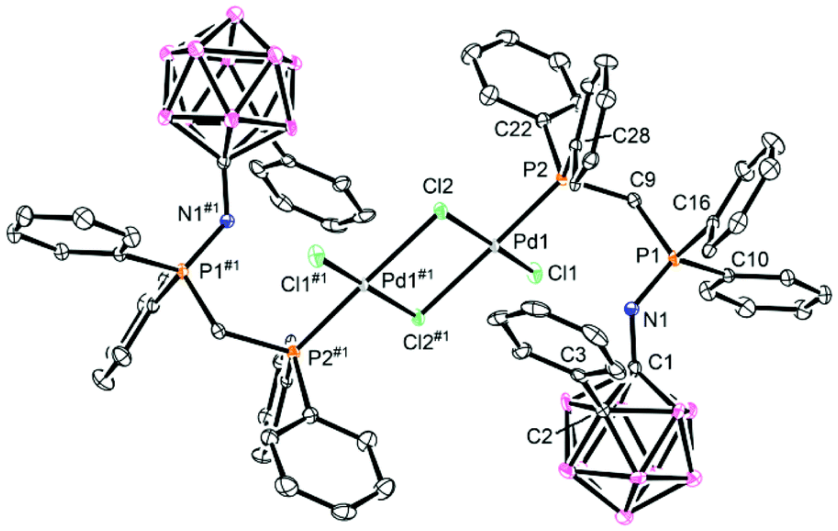

Fig. 5. Molecular structure of compound **Pd3**. Thermal ellipsoids are shown at the 40% probability level. Hydrogen atoms are omitted for clarity.

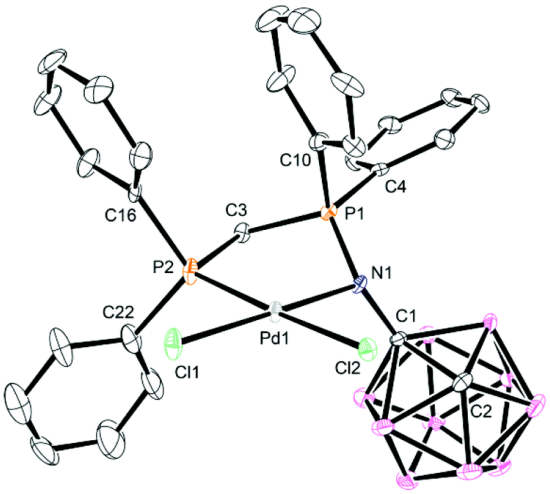

Fig. 6. Molecular structure of compound **Pd1**. Thermal ellipsoids are shown at the 40% probability level. Hydrogen atoms are omitted for clarity.

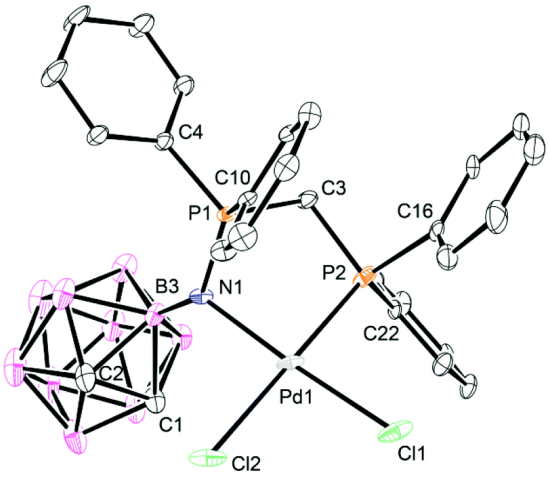

Fig. 7. Molecular structure of compound **Pd4**. Thermal ellipsoids are shown at the 40% probability level. Hydrogen atoms are omitted for clarity.

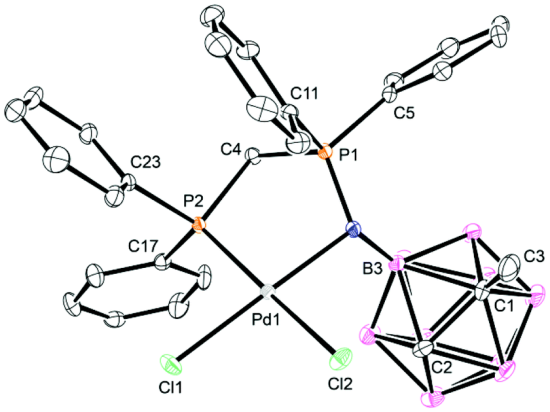

Fig. 8. Molecular structure of compound **Pd5**. Thermal ellipsoids are shown at the 40% probability level. Hydrogen atoms are omitted for clarity.

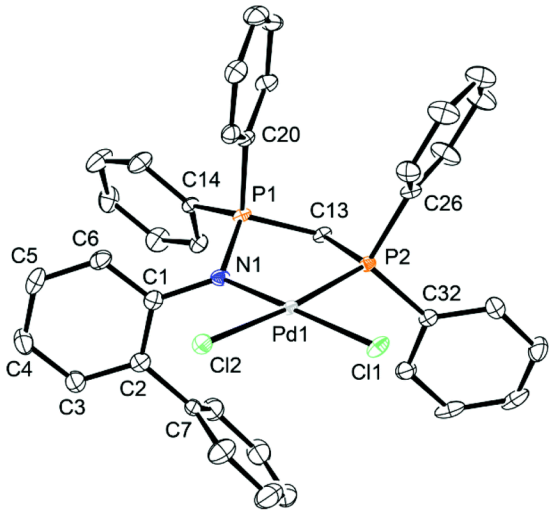

Fig. 9. Molecular structure of compound **Pd6**. Thermal ellipsoids are shown at the 40% probability level. Hydrogen atoms are omitted for clarity.

Table 3. Selected bond lengths (Å) for **Pd1–Pd6**.

	Pd–N	Pd–P	Pd–Cl1	Pd–Cl2	Pd–Cl2$^{\#1}$	P═N	N–Cc/B	Cc–Cc
Pd1[a]	2.132(3)	2.2248(10)	2.2948(9)	2.3725(9)	—	1.628(3)	1.417(4)	1.680(5)
	2.118(3)	2.2219(9)	2.2888(9)	2.3717(9)	—	1.621(3)	1.430(4)	1.665(5)
Pd2	—	2.2099(7)	2.2853(8)	2.3486(8)	2.4209(7)	1.586(2)	1.388(3)	1.769(4)
Pd3	—	2.2120(8)	2.2699(9)	2.3251(8)	2.4210(8)	1.568(3)	1.366(4)	1.786(5)
Pd4	2.103(4)	2.2258(17)	2.3012(16)	2.3878(17)	—	1.606(4)	1.437(8)	1.628(7)
Pd5	2.0972(17)	2.2243(6)	2.2908(6)	2.4023(6)	—	1.6075(18)	1.461(3)	1.623(3)
Pd6	2.059(3)	2.2135(10)	2.2999(10)	2.3789(9)	—	1.605(3)	1.430(4)	—

[a] Two molecules per asymmetric unit. Symmetry transformation used to generate equivalent atoms #1: $-x + 1, -y + 1, -z + 1$ (**Pd2**) and #1: $-x + 1, -y, -z + 1$ (**Pd3**).

Table 4. Selected bond angles (°) for the dimeric complexes **Pd2** and **Pd3**.

	P2–Pd–Cl1	P2–Pd–Cl2	P2–Pd–Cl2$^{\#1}$	Cl1–Pd–Cl2	Cl1–Pd–Cl2$^{\#1}$	Cl2–Pd–Cl2$^{\#1}$	C1/B3–N1–P1
Pd2	92.83(3)	90.37(3)	175.52(3)	170.52(3)	90.70(3)	85.72(3)	127.5(2)
Pd3	86.96(3)	95.09(3)	178.22(3)	172.54(3)	92.43(3)	85.31(3)	132.7(2)

The crystal structures of the palladium complexes can be grouped in two different classes according to the coordination mode of the potential (P, N) donating ligands: (i) dimeric complexes with two P-terminal ligands and (ii) monomeric complexes with one (P, N) chelating ligand.

(i) P-terminal ligands. Compounds **Pd2** (Fig. 4) and **Pd3** (Fig. 5) are neutral dinuclear palladium(ii) complexes with a di-μ-chloro bridge, two equivalent terminal chlorine ligands and two equivalent P-terminal carborane ligands (**L2** and **L3**, respectively). The equivalent ligands are related by an inversion center. The ligands that show this coordination mode are disubstituted C-carboranyl derivatives with a phosphine-iminophosphorane group on one cage carbon atom and a methyl (**L2**) or phenyl (**L3**) group on the other cage carbon atom. The inversion center at the middle point of the line than join the two palladium atoms reflects the planarity of the central $[(\mu\text{-}Cl)_2Pd_2]$ four-membered rings and the *anti*-disposition of the terminal ligands around the central Pd_2Cl_2 unit. Each palladium atom presents a $[PCl_3]$ coordination environment in a distorted square planar geometry. The main source of distortion with respect to the ideal square planar geometry is the formation of the central $[(\mu\text{-}Cl)_2Pd_2]$ ring [Cl–Pd–$Cl^{\#1}$: 85.72(3)° for **Pd2** and 85.31(3)° for **Pd3**]. The coordination plane $[PdPCl_3]$ is essentially planar in both cases [rms: 0.0735 Å (**Pd2**) and 0.0602 Å (**Pd3**)]. Both complexes present the same conformation, with the carborane cages occupying the space above and below the central $[(\mu\text{-}Cl)_2Pd_2]$ ring, and the methyl (**Pd2**) and phenyl (**Pd3**) substituents pointing towards this ring.

Table 5. Selected bond angles (°) for the monomeric complexes **Pd1**, **Pd4**–**Pd6**.

	P–Pd–N	P–Pd–Cl1	P–Pd–Cl2	N–Pd–Cl1	N–Pd–Cl2	Cl1–Pd–Cl2	Cc/B–N–P	Dihedral[b]
Pd1[a]	90.51(8)	86.34(3)	174.51(4)	176.57(8)	92.34(8)	90.91(3)	125.4(2)	4.86(8)
	88.13(8)	88.36(3)	177.73(3)	176.06(8)	92.69(8)	90.89(3)	126.0(2)	2.75(7)
Pd4	89.45(13)	87.18(6)	179.47(6)	176.58(13)	90.68(13)	92.69(7)	125.2(4)	0.79(16)
Pd5	89.95(5)	86.65(2)	171.618(18)	172.74(4)	91.62(5)	92.68(2)	124.30(15)	10.23(4)
Pd6	88.34(9)	87.22(4)	173.40(4)	173.76(9)	91.80(9)	93.11(3)	120.3(2)	7.75(9)

[a] Two molecules per asymmetric unit. [b] Dihedral angle between the PdPN plane and the $PdCl_2$ plane.

In the case of the carboranyl P-terminal ligands, the structural parameters that involve the iminophosphorane nitrogen atom are not affected by the coordination to the palladium atom. The non-coordinated nitrogen atom can engage in *exo*-π-bonding with the carborane cage, which produces the elongation of the Cc–Cc distance and shortens the N–Cc bond.[43] Thus, these compounds show long Cc–Cc distances [1.769(4) for **Pd2** and 1.786(5) Å for **Pd3**] (the longest presented in this paper), and short N–Cc distances [1.388(3) for **Pd2** and 1.366(4) Å for **Pd3**] (the shortest of this paper). The non-coordination of the nitrogen atom is also reflected in the P–N distances of the iminophosphorane groups, which present short values [1.586(2) Å for **Pd2** and 1.568(3) Å for **Pd3**], and also in opened Cc–N–P angles [127.5(2) for **Pd2** and 132.7(2) Å for **Pd3**]. All these parameters (Cc–Cc, N–Cc and P–N distances; Cc–N–P angles) are very similar to those found for the other non-coordinated carboranyl iminophosphorane ligands found in the literature,[12,13,18] especially for the very similar methyl- and phenyl- carborane derivatives of triphenyliminophosphorane.[18]

The Pd–P distances [2.2099(7) for **Pd2** and 2.2120(8) Å for **Pd3**], *trans* to a bridging chlorine atom, are in the expected range for this type of geometry. Similar values are found in other palladium dimers with related terminal phosphines ($Ph_2P–CH_2–$), like for example $[PdCl_2(PPh_2Pr)]_2$, 2.227 Å,[39] or $[PdCl_2(PPh_2CH_2Ph)]_2$, 2.221 Å.[40] The effect of the coordination of the phosphine phosphorus atom to the palladium metal atom is also reflected in the P–C bond distances, but this is only made clear by comparison with data found in the literature for free phosphine-iminophosphorane ligands. The literature only presents four examples of similar free ligands derived from the diphosphine *dppm*.[35] These examples show that the iminophosphorane P(v)–C distances (1.787–1.808 Å)[35] are shorter than the phosphine P(iii)–C distances (1.826–1.864 Å)[35] and that, in

both cases, the distances that involve the phenyl rings are always slightly shorter [P(v)–C(Ph): 1.787–1.806 Å; P(iii)–C(Ph): 1.826–1.839 Å] than the corresponding distances that involve the aliphatic spacer [P(v)–C(CH_2): 1.799–1.808 Å; P(iii)–C(CH_2): 1.853–1.864 Å].[35] In the case of the carboranyl complexes **Pd2** and **Pd3**, although the P(v)–C distances involving the iminophosphorane P atom are almost unaffected by the coordination of the ligand [P(v)–C(Ph): 1.798(3)–1.806(3) Å; P(v)–C(CH_2): 1.815(3) for **Pd2** and 1.820(3) Å for **Pd3**], the P(phosphine)–C distances [P(iii)–C(Ph): 1.799(3)–1.816(3) Å; P(iii)–C(CH_2): 1.824(3) Å for **Pd2** and 1.815(3) Å for **Pd3**] are shorter than those found for the literature free ligands and more similar to P(v)–C distances.

The Pd–Cl bond distances depend on the coordination mode of the chlorine atom and on the donor atom located on *trans* position (*trans* influence). The shortest Pd–Cl distances correspond to the terminal Cl ligand, *trans* to a bridging chlorine atom [2.2853(8) Å for **Pd2** and 2.2699(9) Å for **Pd3**]. The other two Pd–Cl distances are different (asymmetric chloro bridge) due to the different *trans* influence of the phosphine group and the terminal chlorine ligand. The Pd–Cl bond distances *trans* to the phosphine phosphorus atom are longer [2.4209(7) for **Pd2** and 2.4210(8) Å for **Pd3**] and the Pd–Cl bond distances *trans* to the terminal chlorine ligand are shorter, [2.3486(8) Å for **Pd2** and 2.3251(8) Å for **Pd3**]. The same pattern of Pd–Cl distances is found in the literature for similar palladium dimers with terminal phosphines, for example $[PdCl_2(PPh_2Pr)]_2$ [2.268, 2.444 and 2.321 Å, respectively],[39] or $[PdCl_2(PPh_2CH_2Ph)]_2$, [2.273, 2.412 and 2.315 Å, respectively].[40]

In conclusion, the presence of the non-coordinated carboranyl-iminophosphorane moiety does not affect the coordinating abilities of the phosphine group of the ligand, which behaves like a typical terminal phosphine ligand.

(ii) (P, N) chelating ligands. Compounds **Pd1** (Fig. 6), **Pd4** (Fig. 7), **Pd5** (Fig. 8), and **Pd6** (Fig. 9) are neutral monomeric palladium(ii) complexes in which the metal atom is coordinated to two *cis* terminal chlorine ligands and to the phosphorus and nitrogen donor atoms of a chelating phosphine-iminophosphorane ligand (**L1**, **L4**, **L5**, and **L6**, respectively). The carborane ligands that show this coordination mode are the C-carboranyl derivative **L1**, with no other substituents on the cage carbon atoms, and the B3-carboranyl ligands **L4**, with unsubstituted cage carbon atoms, and **L5**, with a methyl group on a Cc atom. The non-carboranyl ligand **L6** synthesized for comparison purposes also provides the (P, N) chelate coordination mode in the palladium complex **Pd6**.

The coordination of the chelating (P, N) ligands gives rise to five-membered chelate rings, which present an envelope disposition. The N1–Pd1–P2–C fragment is planar [rms: 0.0449 and 0.1451 Å for **Pd1**; 0.0673 Å for **Pd4**; 0.0283 Å for **Pd5**; 0.0185 Å for **Pd6**] and forms an angle of 53.19(16)° and 49.83(18)° (**Pd1**), 53.85(23)° (**Pd4**), 50.07(9)° (**Pd5**) and 43.96(16)° (**Pd6**) with the N1–P1–C plane. The coordination of the chelate ligands only produces a small distortion with respect to the regular geometry, which is reflected in P–Pd–N chelate angles in the range 88.13(8)–90.51(8)°. The deviation of the *trans* angles respect to the value of 180° is a reflection of the planarity of the coordination plane, $[PdPNCl_2]$. For example (Table 5), the more distorted *trans* angles [171.618(18)° and 172.74(4)°, **Pd5**] correspond to the structure with a higher dihedral angle between the PdPN plane and the $PdCl_2$ plane [10.23(4)°], while the more regular *trans* angles [179.47(6)° and 176.58(13)°, **Pd4**] correspond to the structure with the lower dihedral angle between these planes [0.79(16)°].

In the case of the complex **Pd5** with a B3–N–P connection and a methyl substituent on one cage carbon atom, the methyl group points away from the coordination plane, while the Cc–H group point to the coordination plane and engage in an intramolecular Cc–H···Cl interaction [*d*(H···Cl): 2.373 Å]. In the case of complex **Pd4**, with a B3–B–P connection and no substituents on the Cc atoms, both Cc–H groups engage in intramolecular Cc–H···Cl interactions [*d*(H···Cl): 2.683 and 2.854 Å].

The Pd–Cl distances are a reflection of the different *trans* influence of the phosphine phosphorus atom and the iminophosphorane nitrogen atom. Thus, the values found for the Pd–Cl distances *trans* to the more donating phosphine phosphorus atom [2.3717(9)–2.4023(6) Å, mean value: 2.3826 Å] are longer than the Pd–Cl distances *trans* to the nitrogen atom [2.2888(9)–2.3012(16) Å, mean value: 2.2951 Å]. These values are similar to the values found for $PdCl_2$ adducts of organic (P, N) chelating phosphine-iminophosphorane ligands (12 structures, CSD), with mean values of 2.371 Å for Pd–Cl(*trans*-P) distances and 2.302 Å for Pd–Cl(*trans*-N) distances.[35–38,46,48,49]

The Pd–P distances that involve the carboranyl ligands (complexes **Pd1**, **Pd4** and **Pd5**) are all very similar [2.2219(9)–2.2258(17) Å, mean value: 2.2242 Å], and the corresponding distance found in **Pd6**, with the organic ligand **L6**, is only slightly shorter, 2.2135(10) Å. The comparison of these distances with those found in the literature for $PdCl_2$ adducts of organic phosphine-iminophosphorane ligands, shows a similar mean value, 2.2266 Å, although in a wider range, 2.203–2.253 Å.[31–34,42,44,45] This result indicates that the carboranyl moiety does not affect the Pd–P interaction to a great extent.

The Pd–N distances found for **Pd1**, **Pd4** and **Pd5** (carboranyl ligands), 2.0972(17)–2.132(3) Å (mean value: 2.1125 Å), are clearly longer than the value found for (non-carboranyl) **Pd6**, 2.059(3), which is similar to the mean value of 2.073 Å found in the literature for the $PdCl_2$ adducts of organic phosphine-iminophosphorane ligands.[31–34,42,44,45] This result indicates that the carboranyl moiety reduces the coordinating ability of the iminophosphorane nitrogen atom.

It is also interesting to compare the structural data of the chelating carboranyl ligands with the data described in the literature for palladium complexes with carboranyl phosphine-iminophosphoranes. The two examples described recently,[13] are palladium complexes with (P, N) *nido*-carboranyl phosphine-iminophosphorane ligands. The Pd–N distances found for these (P, N)-chelating *nido* ligands 2.0447(13) Å (*trans* to a bridging chlorine ligand) and 2.072(4) Å (*trans* to a terminal chlorine ligand), are more similar to the values found for the organic derivatives (see before), indicating that only the *closo*-carboranyl derivatives show the reduction of the donating abilities of the nitrogen atom by effect of the carborane cage.

The (P, N) coordination of the phosphine-iminophosphorane ligands is also reflected in other structural parameters. As mentioned before for the complexes with P-terminal ligands (**Pd2** and **Pd3**), the Pd–P coordination is reflected in the P–C distances, that follow the same pattern. Thus, the coordination reduces the P(phosphine)–C bond distances in comparison to the values found in the literature for free phosphine-iminophosphoranes (see before) [P(iii)–C(Ph): 1.791(4)–1.822(3) Å; P(iii)–C(CH_2): 1.831(6)–1.849(2) Å], but it does not affect the P(iminophosphorane)–C bond distances [P(v)–C(Ph): 1.788(6)–1.800(4) Å; P(v)–C(CH_2): 1.786(4)–1.8128(18) Å]. It is interesting that there are no clear differences among the complexes with carboranyl ligands and the organic analog **Pd6**, showing a similar Pd–P interaction. The Pd–N coordination also affects some structural parameters that involve the nitrogen atom. The coordination of the iminophosphorane nitrogen atom to the metal weakens the P–N bond,[38] which is reflected in P–N bond distances [1.605(3)–1.628(3) Å] that are longer than those found for non-coordinated carboranyl-iminophosphoranes, like the known literature examples [1.5659(17)–1.5870(16) Å],[12,13,18] or the P-terminal complexes **Pd2** [1.586(2) Å] and **Pd3** [1.568(3) Å] described before. A more detailed analysis reveals minor differences among **Pd1**, with the nitrogen atom connected to the cage carbon atom [P–N: 1.621(3), 1.628(3) Å], and **Pd4** [1.606(4) Å] and **Pd5** [1.6075(18) Å], with the nitrogen atom connected to a boron atom [P–N: 1.606(4) and 1.6075(18) Å, respectively]. The slightly shorter values found for the B-carboranyl derivatives are more similar to the value found for the organic analog **Pd6**, 1.605(3) Å, which in turn is similar to the mean value of 1.601 Å found in the literature for palladium complexes with organic (P, N) chelating phosphine-iminophosphoranes (CSD, 22 structures).[30–34,42,44–47] It is interesting to note that complex **Pd1** (Cc–N–P connection) shows a weaker Pd–N interaction than **Pd4**, **Pd5** and **Pd6**, as judged by the Pd–N distances (see before), so the higher P–N elongation is an effect of the C-carboranyl group. This result was not observed in the case of the literature *nido exo*-phosphine-iminophosphoranes, which show a normal

elongation of the P–N bond upon Pd–N coordination [1.6100(14) and 1.611(5) Å],[17] indicating that the higher P–N elongation is an effect of the *closo*-C-carboranyl cage.

In the case of compound **Pd1**, with a Cc–N–P connection, the Pd–N coordination also affects the Cc–Cc and the Cc–N bond distances, as it competes with the *exo*-π bonding to the cage carbon atoms. Thus, the Pd–N coordination leads to shorter Cc–Cc distances [1.665(5), 1.680(5) Å] and longer Cc–N distances [1.417(4), 1.430(4) Å] than those found in the literature for a non-coordinated carboranyl iminophosphorane with no other substituents on the other cage carbon atom, 1.688(3) Å and 1.368(2) Å, respectively.[12] In the case of the complexes **Pd4** and **Pd5** (B3–N–P connection), with no donor atoms on the cage carbon atoms, the Cc–Cc distances are very short [1.628(7) and 1.623(3) Å, respectively], even shorter than the value found for free *o*-carborane [Cc–Cc distance: 1.630 Å].[48] Unexpectedly, the shortest distance, 1.623(3) Å, is found for **Pd5**, with a methyl substituent on a cage carbon atom, while the longest distance, 1.628(7) Å, is found for **Pd4**, with no substituents on Cc atoms. The B3–N distances [1.437(8) for **Pd4** and 1.461(3) Å for **Pd5**] are longer than the mean value of 1.379 Å found for free organic boryl-iminophosphorane ligands (20 structures, CSD).

Finally, the P–N coordination of the chelating carboranyl ligands is also reflected in closed Cc/B3–N–P angles [124.30(15)–126.0(2)°, mean value: 125.2°], compared to the angles found for the P-terminal ligands in **Pd2** [127.5(2)°] and **Pd3** [132.7(2)°]. However, these angles are more opened than the one found for the organic analog **Pd6**, 120.3(2)°, possibly due to the steric bulk of the carborane cage.

Discussion

The Cambridge Structural Database (Version 1.22, 2018) collects 24 crystal structures of palladium complexes with organic (non carboranyl) (P, N) phosphine-iminophosphorane ligands,[30–34,42,44–47] of which 14 are $PdCl_2$ adducts.[31–34,42,44,45] In all cases the ligands behave as (P, N) chelating ligands, regardless the spacer between the donor atoms or the substituent on the iminophosphorane nitrogen atom. The only exceptions are two $PdCl_2$ adducts with P-terminal ligands, although in those cases the P-terminal coordination is forced by the stoichiometry of the complexes, $[PdCl_2(\kappa^1\text{-}P)_2]$ or $[PdCl_2(\kappa^1\text{-}P)(L')]$ where (κ^1-P) is the P-terminal phosphine-iminophosphorane ligand and L′ is a neutral coligand.[44b] Indeed, the same ligands show (P, N) chelate coordination when both coordination sites are available.[44b] The palladium complex **Pd6** presented in this paper, with a (P, N) chelating organic phosphine-iminophosphorane ligand, follows the same trend.

The conclusion that the only known coordination mode for organic phosphine-iminophosphorane ligands is the (P, N) chelation, providing both sites are available, is in line with the structures found for the palladium complexes **Pd1**, **Pd4** and **Pd5**, but in contrast with the P-terminal coordination found for the palladium dimers **Pd2** and **Pd3**. The (P, N) chelating mode found for **Pd1**, **Pd4** and **Pd5** confirms that the phosphine group can promote the coordination of a carboranyl iminophosphorane nitrogen atom,[13] despite its usual reluctance to bind a palladium atom.[12] However, it is interesting to note that the carboranyl ligands maintain their *closo* structure in the final complexes. Thus, the (P, N) coordination does not promote the evolution to *nido* derivatives, as was observed when both donor groups, phosphine and iminophosphorane, were directly attached to the cage carbon atoms.[13] The kind of dimeric structure found for **Pd2** and **Pd3**, with a central $[(\mu\text{-}Cl)_2Pd_2]$ ring and a $[PCl_3]$ coordination environment, is very common for (1 : 1) $PdCl_2$ adducts of monophosphines, but rare for potentially bidentate ligands. Thus, although other potentially (P, N) donating ligands are also known to form this kind of dimers through P-terminal coordination,[49] the nitrogen atom of the iminophosphorane group is always donating enough to promote (P, N) coordination in organic phosphine-iminophosphoranes.

Aiming to rationalize the different structures observed for the **Pd1**–**Pd5** complexes, we performed a density functional theory (DFT) investigation (see computational details below). We started the study by optimizing the structures of the ligands, **L1–L5**. The Mulliken charges of the N atoms calculated using DFT (Table S2, ESI†) reflect the different (electronic) inductive effect of the carboranyl substituents. These charges are clearly more negative for the B-carboranyl ligands **L4** and **L5** (−0.83 and −0.90, respectively) than for the C-carboranyl ones, **L1–L3** (−0.05, −0.24 and +0.16, respectively), which show a rather strong electron-withdrawing effect. The *ν*(PN) stretching frequencies of **L1** and **L2** (1349 and 1357 cm^{-1}) are calculated at lower wavenumbers than those of **L4** and **L5** (1409–1393 cm^{-1}), in line with the experimental data (Table S2†). The natural charges obtained with natural population analysis (NPA) show the same trend, calculating more negative charges for B-carboranyl derivatives (Table S2). This suggests that the higher electron-withdrawing effect of the carborane cage in C-carboranyl derivatives weakens the iminophosphorane bond. The Mulliken charges also show the different inductive effect that the substituents on the cage carbon atoms exert on the nitrogen atom. The calculations confirm the electron-withdrawing effect of the phenyl substituent (**L3**) and the electron-donating character of the methyl group (**L2** and **L5**). However, it is important to note that the inductive effect of the methyl group is higher when the nitrogen atom is connected to the other cage carbon atom (C-carboranyl derivative **L2**) than when it is connected to the B3 boron atom (B-carboranyl derivative **L5**). The natural charges (Table S2) confirm the inductive effect of the methyl and phenyl substituents, although the inductive effect calculated for both groups is less accused. Thus, the calculations show the donating character of the methyl group when connected to a cage carbon atom, which is in contrast with the acceptor character observed when the methyl group is connected to cage boron atoms.[50]

We next performed DFT calculations on the [$PdLCl_2$] complexes (L = **L1–L5**), with the ligand providing a chelating (P,N) coordination. The DFT calculations provide calculated Pd–N distances (Fig. 10) that can be used to estimate the coordinating strength of the nitrogen atom. The calculations show that the derivatives with the iminophosphorane unit at the cage carbon atom (**L1–L3**) present longer Pd–N distances than the B-substituted analogues (**L4**, **L5**), which is in line with the trends in Mulliken charges described above. The calculated Pd–N distances also show the combined electronic and steric effects that the methyl or phenyl substituents on the cage carbon atom induce on the nitrogen donor atom. The much longer Pd–N distance calculated for the hypothetical complex [Pd(**L3**)Cl_2], with a phenyl substituent, is easy to rationalize as both electronic and steric factors cooperate to the elongation of the Pd–N bond. The case of the methyl group is particularly interesting as it leads to longer Pd–N distances compared to the unsubstituted ligands. The higher lengthening calculated for the methyl substituted B-carboranyl ligand **L5**, compared to the substituted C-carboranyl analog **L2**, is a reflection of the different inductive effect of the methyl group, as the steric hindrance is exactly the same in both cases. The better transmission of the donating effect of the methyl group in the C-carboranyl ligand **L2**, as suggested by Mulliken charges of the unbound ligands (see before), compensates its steric hindrance and leads only to a small elongation of the Pd–N distance. In the case of the B-carboranyl analog **L5**, the steric effects determine the final Pd–N distance, as the inductive effect is less accused.

The nature of the Pd–N bonds was also characterized by the values of the electron density at the bond critical points (ρ_{BCP}) and the corresponding Laplacian values ($\nabla^2\rho_{BCP}$).[51] Longer Pd–N distances are associated to lower electron densities at the bond critical points (ρ_{BCP}) and lower Laplacian bond orders (LBOs),[52] reflecting weaker bonds (Table S3, ESI[i]). The positive $\nabla^2\rho_{BCP}$ values obtained for all complexes (0.31–0.34) are typical of Pd–N bonds,[53] and indicate a mostly ionic interaction with a minor covalent contribution suggested by the negative values of the total electron energy density (H(r)).[54] In the case of the B-carboranyl derivatives (**L4** and **L5**) the introduction of a methyl group at a cage carbon atom (**L5**) results in longer Pd–N bonds and lower ρ_{BCP} values, indicating that the substituent hinders the approximation of the N atom to the Pd center. In the C-substituded derivatives **L1** and **L2** the Pd–N bonds are characterized by

nearly identical distances, ρ_{BCP} values and LBOs, reflecting the compensation of the steric hindrance with the electron-donating character, as commented before.

In practice, the B-carboranyl unit, although slightly electron-withdrawing, does not deactivate the coordinating character of the iminophosphorane nitrogen atom to a great extent. The complexes with B-carboranyl ligands, **Pd4** and **Pd5**, show the expected (P, N) chelating coordination, which indicates that the destabilization of the Pd–N interaction by the steric hindrance of the methyl group (**Pd5**) is not enough to prevent the formation of the Pd–N bond. However, in the case of the more electron-withdrawing C-carboranyl analogs **Pd1**–**Pd3**, although the unsubstituted ligand (**Pd1**) can still promote the expected chelate coordination, even the small destabilization induced by the methyl group (**Pd2**) can hinder the formation of the Pd–N bond, preventing the formation of a very stable five-membered chelate ring and forcing a P-terminal coordination of the ligand. The unsubstituted C-carboranyl ligand **L1** seems to mark the limit for the Pd–N bond formation, as further substitution of the other cage carbon atom leads to the total deactivation of the nitrogen coordination capacity, even with small (donating) methyl groups.

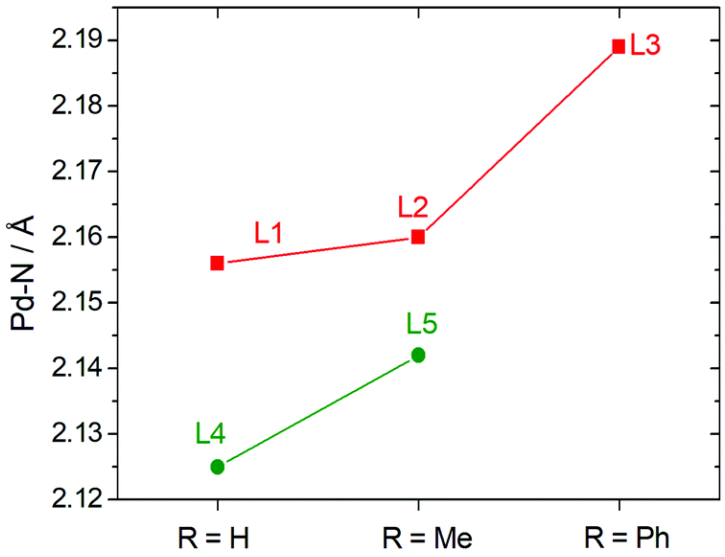

Fig. 10. Pd–N bond distances calculated using DFT for the mononuclear complexes [$PdLCl_2$] with chelating (P,N) ligand coordination. The distances become longer as the steric demand of the substituent at the Cc atom (H, Me or Ph) increases.

The relative stability of both coordination modes was also studied by calculating the relative free energies of the chelating (P,N) species with respect to the dinuclear palladium(ii) complexes with a di-μ-chloro bridge. The results favor the chelating (P,N) coordination by 5.6, 1.7 and 0.1 kcal mol^{-1} for the complexes of **L1**, **L2** and **L3**, respectively. Thus, according to our calculations the introduction of the methyl group stabilizes the dinuclear complex by *ca.* 4 kcal mol^{-1}. The relative free energies of the mononuclear **Pd4** and **Pd5** complexes with respect to the dinuclear complexes with P-terminal coordination favor the mononuclear species by 45.9 and 42.9 kcal mol^{-1}, respectively. The comparison of these energy data with the corresponding values obtained for **Pd1** and **Pd2** (5.6 and 1.7 kcal mol^{-1}) highlights the dramatic effect that the different substitution of the carboranyl moiety (B- or C-substitution) has on the coordinating ability of the N atom.

Conclusions

We have synthesized five new carboranyl phosphine-iminophosphorane ligands with the carboranyl group directly attached to the iminophosphorane nitrogen atom through a cage carbon atom (C-carboranyl derivatives **L1–L3**) or through the B3 boron atom (B-carboranyl derivatives **L4** and **L5**), and the phosphine group on a side chain derived from the diphosphine *dppm*, *i.e.* with a two-atom spacer between the P and N donor atoms (see Fig. 3). The Cc- and B3-carboranyl connections are associated with different electron-withdrawing character, although they present the same steric bulk. Thus, the designed ligands were used to study how the different inductive effect of these substituents can modify the coordinating ability of the nitrogen atom. The experimental results show that although some complexes present the expected (P, N) coordination mode that is always found for non-carboranyl analogs, the disubstituted C-carboranyl ligands **L2** and **L3** present a P-terminal coordination mode in the dimeric palladium complexes **Pd2** and **Pd3**.

The DFT calculations have shown that the (donating) inductive effect of a methyl substituent on a cage carbon atom is better transmitted to a nitrogen donor atom on the other cage carbon atom than to a nitrogen donor atom on the adjacent B3- position, where it mainly acts as a steric group. The calculations also show the great deactivation associated with the C-carboranyl group, which marks the limit for the Pd–N bond formation. The attempts to further modulate the donor strength of the nitrogen atom by substituting the other cage carbon atom (**Pd2** and **Pd3**) resulted in an unexpected change of coordination mode from (P, N) chelating to P-terminal coordination. This indicates that further modulation of the donating strength of the nitrogen atom by functionalization of the other cage carbon atom is not possible. Thus, the B-carboranyl ligands are possibly more versatile, as they can be further functionalized on the cage carbon atoms for a finer tuning of the coordinating strength of the nitrogen atom. The modulation of the deactivation of the nitrogen atom is very important as it can lead to hemilabile behavior, which is very interesting for catalytic applications.

We have shown that the carborane cage can produce different deactivating effects without changing its steric properties. Thus, regardless the point of connection, the carborane cage always retains its bulky character. The large alkyl groups that are generally used to increase the steric bulk around a certain atom are associated with electron-donating character. In contrast, the carborane substituent combines steric bulk with (tuneable) electron-withdrawing character.

Experimental and computational section

Instrumentation

Elemental analysis were performed using a Thermo Finnigan Flash 1112 microanalyzer. Solid state ATR-IR spectra were recorded on a high-resolution spectrometer FT-IR PerkinElmer Spectrum Two. The ^{1}H NMR and ^{31}P NMR spectra were recorded on a Varian Mercury 300 spectrometer. The ^{11}B NMR spectra were recorded on a Varian Inova 500. All NMR spectra were recorded in $CDCl_3$ solutions at 25 °C. Chemical shift values for ^{1}H NMR were referenced to $SiMe_4$ (TMS), those for ^{31}P were referenced to 85% H_3PO_4, and those for $^{11}B\{^{1}H\}$ NMR were referenced to external $BF_3{\cdot}OEt_2$. Chemical shifts are reported in units of parts per million downfield from the reference, and all coupling constants are reported in Hertz. Mass spectra of the ligands **L1–L6** were determined on a Micromass Autospec instrument (positive electronic impact). MALDI-TOF mass spectra of the metal complexes **Pd1–Pd6** were recorded in negative-ion mode on a Bruker Autoflex instrument. In the case of the dimeric complexes **Pd2** and **Pd3**, their mass spectra were also determined in the ESI^{+} mode, on a Bruker Microtof instrument.

Materials

All reactions were performed under atmosphere of dinitrogen employing standard Schlenk techniques. Tetrahydrofuran, acetonitrile and dichloromethane were purchased from Merck and distilled from sodium benzophenone, P_4O_{10} and calcium hydride, respectively, previously to use. Commercial grade diethyl ether, ethyl acetate, hexane, chloroform and dichloromethane were used without further purification. Demineralized water was used in the aqueous stages of synthesis. The precursors tosyl azide,[55] bis(benzonitrile)palladium(ii) chloride, *cis*-[$PdCl_2(PhCN)_2$],[37] and 1-R-3-NH_2-1,2-*ortho*-carborane, R = H, Me,[24,25] were synthesized according to the literature. *o*-Carborane precursors, *o*-1-R-$C_2B_{10}H_{11}$ R = H, Me, Ph, were supplied from KatChem Ltd (Prague) and used as received. The precursors terc-butyl nitrite, trimethylsilyl azide, 2-phenylaniline, bis(diphenylphosphino)methane (*dppm*) and *n*-BuLi solution (1.6 M in hexanes) were purchased from Aldrich and used as received.

Synthesis of C-carboranyl iminophosphoranes, L1–L3

The compounds were synthesized in a similar way, following the literature procedure described for other C-carboranyl iminophosphoranes.[12,13,18]

Synthesis of L1

To a solution of *ortho*-carborane (0.5 g, 3.47 mmol) in dry THF (40 mL) at −10 °C, was added dropwise a solution of *n*-BuLi 1.6 M in hexanes (2.28 mL, 3.65 mmol). The mixture was stirred for 30 minutes and then tosyl azide (0.6 mL, 3.68 mmol) was added. The reaction mixture was stirred at −10 °C for 30 minutes and then 30 minutes at room temperature. A solution of *dppm* (1.43 g, 3.72 mmol) in dry THF (10 mL) was added dropwise. The reaction mixture was heated to reflux for 1.5 hours (evolving nitrogen gas). The cold reaction mixture was evaporated to dryness to yield a brown oil. The crude mixture was purified by silica column chromatography (90 : 10, hexane : ethyl acetate). Yield: 0.798 g (43%); white solid. ^{1}H NMR ($CDCl_3$), δ (ppm): 0.90–2.81 (bm, 10H, B*H*), 3.23 (d, 2H, P-CH_2-P), 3.72 (s, 1H, C_{cage}-*H*), 7.27 (m, 10H, PPh_2), 7.39 (m, 4H, *m*-PPh_2), 7.50 (m, 2H, *p*-PPh_2), 7.58 (m, 4H, *o*-PPh_2) ppm. ^{31}P{^{1}H} NMR ($CDCl_3$) δ (ppm): −30.9 (d, $^2J_{PP}$ = 54.7 Hz, –CH_2*P*Ph_2), 5.9 (d, $^2J_{PP}$ = 54.7 Hz, *P*═N) ppm. ^{11}B NMR ($CDCl_3$) δ (ppm): −15.7, −14.8, −13.3, −12.2, −11.0, −5.9. IR (ATR, ν/cm^{-1}): 3057w, 2613s, 2588vs ν(B–H), 2562vs, 1434vs, 1370s ν(P═N), 1326s, 1307s, 1117s, 1107s, 770s, 692vs. MS (EI, *m*/*z*): 541 (27.8%) $[L]^+$, 464 (66.5%) $[L\text{-}Ph]^+$, 342 (7.5%) $[L\text{-}CH_2PPh_2]^+$, 262 (25.1%) $[PPh_3]^+$, 199 (96.2%) $[CH_2PPh_2]^+$, 185 (56.2%) $[PPh_2]^+$, 121 (100.0%) $[CH_2PPh]^+$. Elemental analysis calcd (%) for $C_{27}H_{33}B_{10}NP_2$: C 59.8, H 6.1, N 2.6; found: C 59.2, H 6.1, N 2.5.

Synthesis of L2

Starting materials: *ortho*-1-Me-carborane (0.5 g, 3.14 mmol); *n*-BuLi 1.6 M in hexanes (2.15 mL, 3.45 mmol); tosyl azide (0.55 mL, 3.45 mmol) and *dppm* (1.39 g, 3.61 mmol). Yield: 0.889 g (51%); white solid. ^{1}H NMR ($CDCl_3$), δ (ppm): 1.12–3.02 (bm, 10H, B*H*), 2.01 (s, 3H, C_{cage}-CH_3), 3.32 (d, 2H, P-CH_2-P), 7.28 (m, 10H, PPh_2), 7.38 (m, 4H, *m*-PPh_2), 7.51 (m, 2H, *p*-PPh_2), 7.63 (m, 4H, *o*-PPh_2) ppm. ^{31}P{^{1}H} NMR ($CDCl_3$) δ (ppm): −30.1 (d, $^2J_{PP}$ = 57.0 Hz, –CH_2*P*Ph_2), 9.1 (d, $^2J_{PP}$ = 57.0 Hz, *P*═N) ppm. ^{11}B NMR ($CDCl_3$) δ (ppm): −14.5, −13.4, −12.7, −12.2, −9.1. IR (ATR, ν/cm^{-1}): 3056w, 2566vs ν(B–H), 1481w, 1433m, 1372w, 1304s ν(P═N), 1121m, 1108m, 1087m, 772m, 741m, 687vs. MS (EI, *m*/*z*): 555 (12.8%) $[L]^+$, 478 (9.8%) $[L\text{-}Ph]^+$, 370 (3.4%) $[L\text{-}PPh_2]^+$, 356 (4.0%) $[L\text{-}CH_2PPh_2]^+$ 276 (100.0%) $[PPh_2\text{-}CH_2Ph]^+$. Elemental analysis calcd (%) for $C_{28}H_{35}B_{10}NP_2$: C 60.5, H 6.3, N 2.5; found: C 59.8, H 6.4, N 2.6.

Synthesis of L3

Starting materials: *ortho*-1-Ph-carborane (0.5 g, 2.26 mmol); *n*-BuLi 1.6 M in hexanes (1.55 mL, 2.49 mmol); tosyl azide (0.39 mL, 2.49 mmol) and *dppm* (1 g, 2.6 mmol). Yield: 0.558 g (40%); white solid. ^{1}H

NMR ($CDCl_3$), δ (ppm): 1.11–3.44 (bm, 10H, B*H*), 2.89 (d, 2H, P-C*H*$_2$-P), 7.14 (m, 4H, *m*-PPh_2), 7.25 (m, 12H: 4H, *o*-PPh_2; 4H, *m*-PPh_2; 4H, *p*-PPh_2), 7.33 (m, 2H, *m*-Ph), 7.42 (m, 4H, *o*-PPh_2), 7.52 (m, 1H, *p*-Ph), 7.70 (m, 2H, *o*-Ph). $^{31}P\{^1H\}$ NMR ($CDCl_3$) δ (ppm): −30.5 (d, $^2J_{PP}$ = 56.6 Hz, –CH_2*P*Ph_2), 7.4 (d, $^2J_{PP}$ = 56.6 Hz, *P*═N) ppm. ^{11}B NMR ($CDCl_3$) δ (ppm): −14.8, −12.6, −11.5, −10.4, −6.5. IR (ATR, ν/cm^{-1}): 3436s, 3058w, 2580s ν(B–H), 1703vw, 1435s, 1375vs ν(P═N), 1115m, 1074m, 1028w, 738s, 692vs. MS (EI, *m*/*z*): 617 (19.1%) $[L]^+$, 540 (13.0%) $[L\text{-}Ph]^+$, 432 (3.0%) $[L\text{-}PPh_2]^+$, 418 (5.4%) $[L\text{-}CH_2PPh_2]^+$, 341 (1.1%) $[L\text{-}(CH_2PPh_2)\text{-}Ph]^+$, 276 (100.0%) $[PPh_2\text{-}CH_2Ph]^+$, 262 (15.3%) $[PPh_3]^+$. Elemental analysis calcd (%) for $C_{33}H_{37}B_{10}NP_2$: C 64.2, H 6.0, N 2.3; found: C 63.6, H 5.8, N 2.4.

Synthesis of B-carboranyl iminophosphoranes, L4 and L5

Synthesis of L4: To a solution of 3-NH_2-1,2-*ortho*-carborane (0.2 g, 1.25 mmol) in dry acetonitrile (40 mL) at 0 °C, was added dropwise *terc*-butyl nitrite (0.22 mL, 1.84 mmol) and trimethylsilyl azide (0.24 mL, 1.84 mmol). The yellow solution was stirred at room temperature for 1.5 hours and then a solution of *dppm* (1.41 g, 3.67 mmol) in dry THF (10 mL) was added dropwise. The reaction mixture was heated to reflux for 2 hours (evolving nitrogen gas). The cold reaction mixture was evaporated to dryness to yield a brown oil which was purified by silica column chromatography (90 : 10, hexane : ethyl acetate). Yield: 0.462 g (67%); white solid. ^1H NMR ($CDCl_3$) δ (ppm): 1.20–2.76 (bm, 10H, B*H*), 3.03 (bs, 2H, C_{cage}-*H*), 3.17 (d, 2H, P-C*H*$_2$-P), 7.30 (m, 6H, 2H, *p*-PPh_2, 4H, *m*-PPh_2), 7.38 (m, 4H, *o*-PPh_2), 7.43 (m, 4H, *m*-PPh_2), 7.50 (m, 2H, *p*-PPh_2), 7.71 (m, 4H, *o*-PPh_2). $^{31}P\{^1H\}$ NMR ($CDCl_3$) δ (ppm): −30.2 (d, $^2J_{PP}$ = 50.8 Hz, –CH_2-*P*Ph_3), 5.8 (d, $^2J_{PP}$ = 50.8 Hz, *P*═N). ^{11}B NMR ($CDCl_3$) δ (ppm): −23.3, −17.1, −15.3, −13.6, −7.5, 1.3. IR (ATR, ν/cm^{-1}): 3071w, 3058w, 2586s, ν(B–H) 2560s ν(B–H), 1586vw, 1480vs, 1433vs ν(P═N), 1133w, 1108m, 1025w, 980w, 773m, 747m, 736m, 721m, 692s, 615w, 531m, 498m. MS (EI, *m*/*z*): 540 (67.6%) $[L]^+$, 462 (72.4%) $[L\text{-}Ph]^+$, 356 (15.7%) $[L\text{-}PPh_2]^+$, 342 (52.0%) $[L\text{-}CH_2PPh_2]^+$, 262 (67.1%) $[PPh_3]^+$, 185 (21.0%) $[PPh_2]^+$. Elemental analysis calcd (%) for $C_{27}H_{33}B_{10}NP_2$: C 60.2, H 6.1, N 2.6; found: C 60.2, H 6.3, N 2.4.

Synthesis of L5: *Starting materials:* 1-Me-3-NH_2-1,2-*ortho*-carborane (0.2 g, 1.15 mmol); *tert*-butyl nitrite (0.22 mL, 1.84 mmol); trimethylsilyl azide (0.24 mL, 1.80 mmol); and *dppm* (0.75 g, 1.95 mmol). Yield: 0.421 g (66%); white solid. ^1H NMR ($CDCl_3$) δ (ppm): 1.12–2.50 (bm, 9H, B*H*), 1.90 (s, 3H, C_{cage}-C*H*$_3$), 2.69 (bs, 1H, C_{cage}-*H*), 3.22 (t, 1H, P-C*H*$_2$-P), 3.32 (t, 1H, P-C*H*$_2$-P), 7.30 (m, 4H, *m*-PPh_2), 7.38 (m, 2H, *p*-PPh_2), 7.44 (m, 8H, 4H *o*-PPh_2, 4H *m*-PPh_2), 7.52 (m, 2H, *p*-PPh_2), 7.78 (m, 4H, *o*-PPh_2). $^{31}P\{^1H\}$ NMR ($CDCl_3$) δ (ppm): −29.9 (d, $^2J_{PP}$ = 52.7 Hz, CH_2-*P*Ph_3), 8.1 (d, $^2J_{PP}$ = 52.7 Hz, *P*═N). ^{11}B NMR ($CDCl_3$) δ (ppm): −22.2, −17.4, −14.8, −13.8, −12.9, −10.6, −8.0, 2.0.IR (ATR, ν/cm^{-1}): 3055w; 2571s ν(B–H); 2147m; 1480m; 1433s; 1403s; 1374s ν(P═N); 1113m; 1026m; 997m; 771m; 735vs; 691vs; 530m; 500s. MS (EI, *m*/*z*): 555 (21.6%) $[L]^+$, 478 (20.6%) $[L\text{-}Ph]^+$, 370 (4.3%) $[L\text{-}PPh_2]^+$, 356 (9.1%) $[L\text{-}CH_2PPh_2]^+$, 276 (100.0%) $[N{=}PPh_3]^+$, 262 (42.9%) $[PPh_3]^+$, 185 (11.0%) $[PPh_2]^+$. Elemental analysis calcd (%) for *para* $C_{28}H_{35}B_{10}NP_2$: C 60.5, H 6.3, N 2.5; found: C 59.3, H 6.2, N 2.6.

Synthesis of non-carboranyl iminophosphorane L6

The non-carboranyl derivative **L6** was obtained following the same procedure used for the preparation of the B-carboranyl derivatives, starting from 2-phenylaninile.

Synthesis of L6: *Starting materials:* 2-phenylaniline (0.3 g, 1.77 mmol); *tert*-butyl nitrite (0.25 mL, 2.12 mmol); trimethylsilyl azide (0.28 mL, 2.12 mmol); and *dppm* (1.02 g, 2.65 mmol). Purification: silica column chromatography (80 : 20, hexane : ethyl acetate) Yield: 0.52 g (53%); white solid. ^1H NMR ($CDCl_3$), δ (ppm): 3.27 (bd, 2H, P-C*H*$_2$-P), 6.45 (bd, 1H, *H*$_{Ar}$), 6.75 (t, 1H, *H*$_{Ar}$), 6.86 (m, 1H, *H*$_{Ar}$), 7.16 (m, 4H, *m*-PPh_2), 7.22 (m, 5H, *H*$_{Ar}$), 7.28 (m, 3H, *m*-Ph), 7.34 (m, 4H, *H*$_{Ar}$), 7.41 (m, 5H, *H*$_{Ar}$), 7.71 (m, 3H, *H*$_{Ar}$), 7.79 (m, 2H, *H*$_{Ar}$). $^{31}P\{^1H\}$ NMR ($CDCl_3$) δ (ppm): −29.6 (d, $^2J_{PP}$ = 52.0 Hz, –CH_2*P*Ph_2), −1.2 (d, $^2J_{PP}$ = 52.0 Hz, *P*═N) ppm. IR (ATR, ν/cm^{-1}): 3050w; 2959vw; 1585w; 1473s; 1429s ν(P═N); 1328m; 1285m; 1117;

1061m; 1023m; 998w; 796w; 771m; 731s; 691vs; 613w; 570m; 521m; 494s. MS (EI, *m*/*z*): 551 (100.0%) $[L]^+$, 474 (67.1%) $[L\text{-}Ph]^+$, 352 (60.3%) $[L\text{-}(CH_2PPh_2)]^+$, 199 (40.4%) $[CH_2PPh_2]^+$. Elemental analysis calcd (%) for $C_{24}H_{19}NPBr$: C 80.6, H 5.7, N 2.5; found: C 81.1, H 5.9, N 2.3.

Synthesis of the palladium complexes, Pd1–Pd6

Synthesis of Pd1: To a solution of the metal precursor bis(benzonitrile)palladium(ii) chloride, $[PdCl_2(PhCN)_2]$ (106 mg, 0.28 mmol) in dry acetonitrile (15 mL), was added dropwise a solution of ligand **L1** (150 mg, 0.28 mmol) in dry dichloromethane (10 mL). The reaction mixture was stirred overnight (16 hours) at room temperature. The mixture was concentrated to half of its volume under reduced pressure. Commercial hexane (5 mL) was added to the solution, precipitating a yellow solid. The solid was filtered, washed with diethyl ether and dried under vacuum. Yield: 50 mg (26%), yellow solid. ^{1}H NMR ($CDCl_3$) δ (ppm): 0.89–2.79 (bm, 10H, B*H*), 4.04 (m, 2H, P-C*H*$_2$-P), 5.15 (bs, 1H, C_{cage}-*H*), 7.50 (m, 20H, H_{Ar}) ^{31}P{^{1}H} NMR ($CDCl_3$) δ (ppm): 8.2 (d, $^2J_{PP}$ 32.7 Hz, CH_2-*P*Ph_2), 38.2 (d, $^2J_{PP}$ 32.7 Hz, *P*═N). ^{11}B NMR ($CDCl_3$) δ (ppm): −13.0, −11.6, −10.7, −10.1, −9.3, −8.2. IR (ATR, ν/cm^{-1}): 3434s, 3055w, 2958w, 2864w, 2581s ν(B–H), 1706vw, 1627w, 1462s, 1436vs, 1385m, 1238m ν (P═N), 1159m, 1112s, 1070m, 1021m, 875m, 772w, 732m, 690m, 648vw, 600w, 530w, 503w, 482w. MS (MALDI, *m*/*z*): 682.1 [PdLCl–H], 541.7 [L]. Elemental analysis calcd (%) for $C_{27}H_{33}B_{10}NP_2Cl_2Pd$: C 45.0, H 4.6, N 1.9, found: C 44.6, H 4.8, N 1.8.

Synthesis of Pd2: Starting materials: bis(benzonitrile)palladium(ii) chloride (104 mg, 0.27 mmol) and ligand **L2** (150 mg, 0.27 mmol). Yield: 53 mg (27%); yellow solid. ^{1}H NMR ($CDCl_3$) δ (ppm): 0.78–2.90 (bm, 10H, B*H*), 1.27 (s, 3H, C_{cage}-C*H*$_3$), 2.20 (s, 2H, P-C*H*$_2$-P), 7.34 (m, 6H, 4H *m*-PPh_2 + 2H *p*-PPh_2), 7.52 (m, 8H, 4H *o*-PPh_2 + 4H *m*-PPh_2), 7.65 (m, 6H, 2H *p*-PPh_2 + 4H *o*-PPh_2). ^{31}P{^{1}H} NMR ($CDCl_3$) δ (ppm): 17.5 (d, $^3J_{PP}$ = 8.6 Hz, *P*═N), 20.5 (d, $^2J_{PP}$ = 8.6 Hz, –CH_2*P*Ph_2). ^{11}B NMR ($CDCl_3$) δ (ppm): −17.1, −14.8, −12.1, −5.6, −3.9. IR (ATR, ν/cm^{-1}): 3056w, 2926m, 2854w, 2580s ν(B–H), 1437s, 1336m ν(P═N), 1104m, 1027w, 777w, 740w, 691m. MS (MALDI, *m*/*z*): 697.1 [PdLCl–H], 555.5 $[L]^+$. MS (ESI, *m*/*z*): 1393.4 $[Pd_2L_2Cl_2]^+$, 607.2 $[PdLCl–H]^+$. Elemental analysis calcd (%) for $C_{28}H_{35}NP_2B_{10}Cl_2Pd$: C 45.9, H 4.8, N 1.9, found: C 45.0, H 4.7, N 2.1.

Synthesis of Pd3: Starting materials: bis(benzonitrile)palladium(ii) chloride (62 mg, 0.16 mmol) and ligand **L3** (100 mg, 0.16 mmol). Yield: 64 mg (31%); yellow solid. ^{1}H NMR ($CDCl_3$) δ (ppm): 1.07–3.27 (bm, 10H, B*H*), 3.68 (t, 2H, P-C*H*$_2$-P), 7.20 (m, 4H), 7.31 (m, 8H), 7.47 (m, 6H), 7.54 (m, 4H) 7.62 (m, 1H), 7.67 (m, 2H). ^{31}P{^{1}H} NMR ($CDCl_3$) δ (ppm): 2.1 (d, $^2J_{PP}$ 13.9 Hz, *P*═N), 20.6 (d, $^2J_{PP}$ 13.9 Hz, CH_2-*P*Ph_2). ^{11}B NMR ($CDCl_3$) δ (ppm): −13.2, −11.6, −8.3. IR (ATR, ν/cm^{-1}): 3057w, 2923w, 2852w, 2586s ν(B–H), 2551s ν(B–H), 1587w, 1483w, 1434m, 1396vs ν(P═N), 1189w, 1160m, 1103m, 1073m, 1000w, 796w, 771m, 741s, 715m, 687s, 540w, 502m, 481w. MS (MALDI, *m*/*z*): 759.2 [PdLCl–H], 616.3 $[L]^+$. MS (ESI, *m*/*z*): 1554.4 $[Pd_2L_2Cl_3]^+$. Elemental analysis calcd (%) for $C_{66}H_{74}B_{20}N_2P_4Cl_4Pd_2$: C 49.8, H 4.7, N 1.8, found: C 49.7, H 4.9, N 1.8.

Synthesis of Pd4: Starting materials: bis(benzonitrile)palladium(ii) chloride (71 mg, 0.18 mmol) and ligand **L4** (100 mg, 0.18 mmol). Yield: 48 mg (37%); yellow solid. ^{1}H NMR ($CDCl_3$) δ (ppm): 1.08–2.58 (bm, 10H, B*H*), 3.71 (m, 2H, P-C*H*$_2$-P), 5.16 (bs, 2H, C_{cage}*H*), 7.36 (m, 4H, *m*-PPh_2), 7.50 (m, 6H, 4H *o*-PPh_2, 2H *p*-PPh_2), 7.67 (m, 6H, 2H *p*-PPh_2, 4H *m*-PPh_2), 7.86 (m, 4H, *o*-PPh_2). ^{31}P{^{1}H} NMR ($CDCl_3$) δ (ppm): 11.4 (d, $^2J_{PP}$ 27.6 Hz, CH_2-*P*Ph_2), 40.9 (d, $^2J_{PP}$ 27.6 Hz, *P*═N) ^{11}B NMR ($CDCl_3$) δ (ppm): −17.9, −15.3, −12.1, −5.5, −1.2. IR (ATR, ν/cm^{-1}): 3038m, 2953w, 2900w, 2587s ν(B–H), 2569s ν(B–H), 1484w, 1436s, 1253vs ν(P═N), 1197w, 1118s, 1101s, 1023m, 989m, 971m, 878w, 765m, 732vs, 686s, 593w, 525w, 502w, 481w. MS (MALDI, *m*/*z*): 1401 $[Pd_2L_2Cl_3–H]$, 717 $[PdLCl_2]$, 683 [PdLCl–H]. Elemental analysis calcd (%) for $C_{27}H_{33}B_{10}NP_2Pd\ Cl_2$: C 45.1, H 4.6, N 1.9, found: C 45.8, H 4.8, N 1.8.

Synthesis of Pd5: Starting materials: bis(benzonitrile)palladium(ii) chloride (69 mg, 0.18 mmol) and ligand **L5** (100 mg, 0.18 mmol). Yield: 41 mg (31%); yellow solid. ^{1}H NMR ($CDCl_3$) δ (ppm): 1.07–3.27

(bm, 10H, BH), 2.11 (s, 3H, C_{cage}–CH_3), 3.13 (t, 1H, P-CH_2-P), 4.46 (m, 1H, P-CH_2-P), 6.05 (bs, 1H, C_{cage}-*H*), 7.12 (m, 2H), 7.37 (m, 4H), 7.51 (m, 3H), 7.57 (m, 3H), 7.66 (m, 5H), 8.02 (m, 3H). $^{31}P\{^1H\}$ NMR ($CDCl_3$) δ (ppm): 9.6 (d, $^2J_{PP}$ = 28.4 Hz, CH_2PPh_2), 40.8 (d, $^2J_{PP}$ = 28.4 Hz, *P*═N). ^{11}B NMR ($CDCl_3$) δ (ppm): −16.6, −12.7, −9.9, −6.8, −4.1, −0.4. IR (ATR, ν/cm^{-1}): 2984m, 2904w, 2571m ν(B–H), 2544m ν(B–H), 1587w, 1483w, 1437m, 1383w, 1364w, 1222s ν(P═N), 1121m, 1098m, 1027w, 998m, 955m, 877m, 784m, 747s, 728vs, 686vs, 596m, 551m, 530m, 501s, 481s. MS (MALDI, *m*/*z*): 697 [PdLCl–H], 555 [L]. Elemental analysis calcd (%) for $C_{28}H_{35}B_{10}NP_2PdCl_2$: C 45.9, H 4.8, N 1.9, found: C 46.6, H 5.0, N 1.7.

Synthesis of Pd6: Starting materials: bis(benzonitrile)palladium(ii) chloride (70 mg, 0.18 mmol) and ligand **L6** (100 mg, 0.18 mmol). Yield: 62 mg (47%); yellow solid. ^1H NMR ($CDCl_3$) δ (ppm): 2.79 (t, 1H, P-CH_2-P), 3.00 (m, 1H, P-CH_2-P), 6.98 (m, 3H), 7.07 (m, 2H), 7.13 (m, 2H), 7.21 (m, 5H), 7.31 (m, 2H), 7.43 (m, 4H), 7.54 (m, 7H), 7.68 (d, 2H), 8.02 (m, 2H). $^{31}P\{^1H\}$ NMR ($CDCl_3$) δ (ppm): 12.9 (d, $^2J_{PP}$ = 35.2 Hz, CH_2PPh_2), 41.7 (d, $^2J_{PP}$ = 35.2 Hz, *P*═N). IR (ATR, ν/cm^{-1}): 3057w, 2966w, 2920w, 1588w, 1472w, 1346w, 1271m ν(P═N), 1233w, 1190vw, 1162vw, 1131w, 1112m, 1053w, 1028w, 1007w, 999w, 917vw, 863vw, 816m, 784m, 766m, 746s, 732vs, 686s, 632w, 613w, 535m, 505s, 494m, 473s. MS (MALDI, *m*/*z*): 1421 (7.8%) $[Pd_2L_2Cl_3–H]^+$, 694 (100.0%) $[PdLCl–H]^+$. Elemental analysis calcd (%) for $C_{37}H_{31}NP_2PdCl_2$: C 61.0, H 4.3, N 1.9, found: C 60.8, H 4.2, N 2.0.

X-ray crystallography

Intensity data sets for all compounds were collected with the use of a Bruker X8 Kappa APEXII diffractometer (Mo Kα radiation, λ = 0.71073 Å) equipped with a graphite monochromator. All crystals were measured at 100 K. The omega and phi scans technique was employed to measure intensities in all crystals. No decomposition of the crystals occurred during data collection. The intensities of all data sets were corrected for Lorentz and polarization effects. Absorption effects in all compounds were corrected using the program SADABS.[56] The crystal structures of all compounds were solved by direct methods. Crystallographic programs used for structure solution and refinement were those of SHELXL-2014[57] installed on a PC clone. Scattering factors were those provided with the SHELX program system. Missing atoms were located in the difference Fourier map and included in subsequent refinement cycles. The structures were refined by full-matrix least-squares refinement on F^2, using anisotropic displacement parameters for all non-hydrogen atoms. Hydrogen atoms were placed geometrically and refined using a riding model, including free rotation about C–C bonds for methyl groups, with C–H distances of 0.95–0.99 Å and B–H distances of 1.12 Å. For all compounds, hydrogen atoms were refined with U_{iso} constrained at 1.2 (for non-methyl groups) and 1.5 (for methyl groups) times U_{eq} of the carrier C or B atom. The crystal structure of **Pd1** contains two acetonitrile molecules per asymmetric unit, one of them disordered over two positions. The disorder was handled by introducing split positions in the refinement with the respective occupancies (80/20). This structure also contains a fraction of another molecule of acetonitrile (20%). This crystal structure contains 2 palladium complexes per asymmetric unit; one of them presents an 85/15 disordered phenyl ring. The crystal structures of **Pd2** and **Pd3** contain two and one dichloromethane molecules, respectively, per asymmetric unit. The crystal structure of **Pd4** contains half molecule of dichloromethane per asymmetric unit. Three phenyl rings of the PPh_2 moieties are disordered over two positions, all of them with 50/50 occupancies. The crystal structure of **Pd6** contains two molecules of chloroform per asymmetric unit.

Table S1 (ESI[i]) summarizes pertinent details of the data collection and the structure refinement of the crystal structures. The program ORTEP3[58] was used to generate the pictures of all the molecular structures. CCDC reference numbers: 1855597–1855602.

Computational details

Full geometry optimizations of ligands **L1–L5** were performed within the hybrid-*meta* GGA approximation to DFT employing the TPSSh functional (10% exchange)[59] and the standard 6-31+G(d,p) basis set. The Pd complexes were optimized using the same computational approach together with the relativistic effective core potential of Dolg (ECP28MDF),[60] which includes 28 electrons in the core ([Ar]3d^{10}). The valence space 4s4p4d5s5p was described by the cc-pVDZ-PP basis set, which presents a (25s22p13d1f)/[4s4p3d1f] contraction scheme.[60] The ECP28MDF/cc-pVDZ-PP approximation was found to provide good results for different Pd complexes.[61] Due to the large computational effort required for the calculation of second derivatives, the calculations performed on the dinuclear complexes were carried out using the smaller 6-31G(d) basis set for the ligand atoms. No symmetry constraints were imposed during the optimizations. All stationary points found on the potential energy surfaces as a result of geometry optimizations were characterized by frequency analysis to confirm that they correspond to true energy minima. Wave function analysis (ρ_{BCO}, $\nabla\rho$, $H(r)$ and LBO) was carried out with the computer program Multiwfn 3.2.[62]

Conflicts of interest

There are no conflicts to declare.

Acknowledgements

This work was supported by Xunta de Galicia (Spain) (grant no. 10PXIB209285PR).

References

01 R. N. Grimes, *Carboranes*, Academic Press, London, UK, 2nd edn, 2011.

02 (*a*) M. Y. Tsang, S. Rodríguez-Hermida, K. C. Stylianou, F. Tan, D. Negi, F. Teixidor, C. Viñas, D. Choquesillo-Lazarte, C. Verdugo-Escamilla, M. Guerrero, J. Sort, J. Juanhuix, D. Maspoch and J. G. Planas, *Cryst. Growth Des.*, 2017, **17**, 846–857 and references therein; (*b*) R. Núñez, I. Romero, F. Teixidor and C. Viñas, *Chem. Soc. Rev.*, 2016, **45**, 5147–5173; (*c*) M. Patel, A. C. Swain, A. R. Skinner, L. G. Mallinson and G. F. Hayes, *Macromol. Symp.*, 2003, **202**, 47–58; (*d*) E. N. Peters, *Ind. Eng. Chem. Prod. Res. Dev.*, 1984, **23**, 28–32; (*e*) A. Gonzalez-Campo, R. Núñez, F. Teixidor and B. Boury, *Chem. Mater.*, 2006, **18**, 4344–4353; (*f*) A. Ferrer-Ugalde, E. J. Juarez-Perez, F. Teixidor, C. Viñas and R. Nunez, *Chem. – Eur. J.*, 2013, **19**, 17021–17030; (*g*) O. K. Farha, A. M. Spokoyny, K. L. Mulfort, M. F. Hawthorne, C. A. Mirkin and J. T. Hupp, *J. Am. Chem. Soc.*, 2007, **129**, 12680–12681.

03 (*a*) F. Issa, M. Kassiou and L. M. Rendina, *Chem. Rev.*, 2011, **111**, 5701–5722; (*b*) M. Scholz and E. Hey-Hawkins, *Chem. Rev.*, 2011, **111**, 7035–7062.

04 J. G. Planas, F. Teixidor and C. Viñas, *Crystals*, 2016, **6**, 50–71.

05 (*a*) W. Li, X. Yan, H. Zhang, R. He, M. Li and W. Shen, *Eur. J. Inorg. Chem.*, 2018, 99–108; (*b*) K. O. Kirlikovali, J. C. Axtell, A. Gonzalez, A. C. Phung, S. I. Khan and A. M. Spokoyny, *Chem. Sci.*, 2016, **7**, 5132–5138; (*c*) X. Li, H. Yan and Q. Zhao, *Chem. – Eur. J.*, 2016, **22**, 1888–1898; (*d*) A. Ferrer-Ugalde, A. González-Campo, C. Viñas, J. Rodríguez-Romero, R. Santillan, N. Farfán, R. Sillanpää, A. Sousa-Pedrares, R. Núñez and F. Teixidor, *Chem. – Eur. J.*, 2014, **20**, 9940–9951.

06 (*a*) V. I. Bregadze, *Chem. Rev.*, 1992, **92**, 209–223; (*b*) L. I. Zakharkin and V. A. Ol'shevskaya, *Zh. Obshch. Khim.*, 1987, **57**, 368–372; (*c*) J. Plesek and S. Hermanek, *Collect. Czech. Chem. Commun.*, 1979, **44**, 24–33; (*d*) J. Plesek, S. Hermanek and B. Stibr, *J. Less-Common Met.*, 1979, **67**, 225–228 .

07 K. Hermansson, M. Wójcik and S. Sjölberg, *Inorg. Chem.*, 1999, **38**, 6039–6048.

08 (*a*) R. A. Wiesboeck and M. F. Hawthorne, *J. Am. Chem. Soc.*, 1964, **86**, 1642–1643; (*b*) B. Wrackmeyer, E. V. Klimkina, W. Milius, T. Bauer and R. Kempe, *Chem. – Eur. J.*, 2011, **17**, 3238–3251; (*c*) M. A. Fox, W. R. Gill, P. L. Herbertson, J. A. H. MacBride and K. Wade, *Polyhedron*, 1996, **15**, 565–571; (*d*) M. A. Fox and K. Wade, *J. Organomet. Chem.*, 1999, **573**, 279–291; (*e*) T. D. Getman, *Inorg. Chem.*, 1998, **37**, 3422–3423; (*f*) J. Yoo, J. W. Hwang and Y. Do, *Inorg. Chem.*, 2001, **40**, 568–570; (*g*) A. F. Armstrong and J. F. Valliant, *Inorg. Chem.*, 2007, **46**, 2148–2158; (*h*) H. Lee, T. Onak, J. Jaballas, U. Tran, T. U. Truong and H. T. To, *Inorg. Chim. Acta*, 1999, **289**, 11–19.

09 (*a*) J. Li and M. A. Jones Jr., *Inorg. Chem.*, 1990, **29**, 4162–4163; (*b*) C. Viñas, G. Barberá, J. M. Oliva, F. Teixidor, A. J. Welch and G. M. Rosair, *Inorg. Chem.*, 2001, **40**, 6555–6562; (*c*) H. Yamazaki, K. Ohta and Y. Endo, *Tetrahedron Lett.*, 2005, **46**, 3119–3122; (*d*) S. Robertson, D. Ellis, T. D. McGrath, G. M. Rosair and A. J. Welch, *Polyhedron*, 2003, **22**, 1293–1301; (*e*) W. Chen, J. J. Rockwell, C. B. Knobler, D. E. Harwell and M. F. Hawthorne, *Polyhedron*, 1999, **18**, 1725–1734; (*f*) A. V. Safronov, N. I. Shlyakhtina and M. F. Hawthorne, *Organometallics*, 2012, **31**, 2764–2769; (*g*) M. F. Hawthorne and P. A. Wegner, *J. Am. Chem. Soc.*, 1968, **90**, 896–901.

10 (*a*) A. R. Popescu, F. Teixidor and C. Viñas, *Coord. Chem. Rev.*, 2014, **269**, 54–84; (*b*) A. M. Spokoyny, C. D. Lewis, G. Teverovskiy and S. L. Buchwald, *Organometallics*, 2012, **31**, 8478–848 and references therein; (*c*) A. R. Popescu, A. Laromaine, F. Teixidor, R. Sillanpää, R. Kivekäs, J. I. Llambias and C. Viñas, *Chem. – Eur. J.*, 2011, **17**, 4429–4443.

11 A. M. Spokoyny, C. W. Machan, D. J. Clingerman, M. S. Rosen, M. J. Wiester, R. D. Kennedy, C. L. Stern, A. A. Sarjean and C. A. Mirkin, *Nat. Chem.*, 2011, **3**, 590–596.

12 P. Crujeiras, J. L. Rodríguez-Rey and A. Sousa-Pedrares, *Dalton Trans.*, 2017, **46**, 2572–2593.

13 P. Crujeiras, J. L. Rodríguez-Rey and A. Sousa-Pedrares, *Eur. J. Inorg. Chem.*, 2017, 4653–4667.

14 (*a*) E. I. Matrosov, V. A. Gilyarov, V. Yu. Kovtun and M. I. Kabachnik, *Izv. Akad. Nauk Az. SSR*, 1971, **6**, 1162–1168; (*b*) V. Yu. Kovtun, V. A. Gilyarov, B. A. Korolev, E. I. Matrosov and M. I. Kabachnik, *Zh. Obshch. Khim.*, 1971, **41**, 772–778.

15 J. García-Álvarez, S. E. García-Garrido and V. Cadierno, *J. Organomet. Chem.*, 2014, **751**, 792–808, and references therein.

16 (*a*) S. Ramírez-Rave, F. Estudiante-Negrete, R. A. Toscano, S. Hernández-Ortega, D. Morales-Morales and J. M. Grévy, *J. Organomet. Chem.*, 2014, **749**, 287–295; (*b*) M. Alajarin, C. Lopez-Leonardo, P. Llamas-Lorente, R. Raja, D. Bautista and R. A. Orenes, *Dalton Trans.*, 2012, **41**, 12259–12269.

17 M. G. Davidson, M. A. Fox, T. G. Hibbert, J. A. K. Howard, A. Mackinnon, I. S. Neretin and K. Wade, *Chem. Commun.*, 1999, 1649–1650.

18 R. D. Kennedy, *Chem. Commun.*, 2010, **46**, 4782–4784.

19 J. Estrada, C. A. Lugo, S. G. McArthur and V. Lavallo, *Chem. Commun.*, 2016, **52**, 1824–1826.

20 (*a*) H. Staudinger and J. Meyer, *Helv. Chim. Acta*, 1919, **2**, 619–635; (*b*) H. Staudinger and J. Meyer, *Helv. Chim. Acta*, 1919, **2**, 635–646.

21 R. J. Blanch, L. C. Bush and M. Jones Jr., *Inorg. Chem.*, 1994, **33**, 198–199.

22 D. Zhao and Z. Xie, *Chem. Sci.*, 2016, **7**, 5635–5639.

23 K. Barral, A. D. Moorhouse and J. E. Moses, *Org. Lett.*, 2007, **9**, 1809–1811.

24 J. F. Valliant and P. Schaffer, *J. Inorg. Biochem.*, 2001, **85**, 43–51.

25 (*a*) L. I. Zakharkin, V. N. Kalinin and V. V. Gedymin, *J. Organomet. Chem.*, 1969, **16**, 371–379; (*b*) R. A. Kasar, G. M. Knudsen and S. B. Kahl, *Inorg. Chem.*, 1999, **38**, 2936–2940.

26 (*a*) A. S. Nuraeva, D. S. Vasileva, S. G. Vasilev, P. S. Zelenovskiy, D. A. Gruzdev, V. P. Krasnov, V. A. Olshevskaya, V. N. Kalinin and V. Ya. Shur, *Ferroelectrics*, 2016, **496**, 1–9; (*b*) G. L. Levit, V. P. Krasnov, D. A. Gruzdev, A. M. Demin, I. V. Bazhov, L. Sh. Sadretdinova, V. A. Olshevskaya, V. N. Kalinin, C. S. Cheong, O. N. Chupakhin and V. N. Charushin, *Collect. Czech. Chem. Commun.*, 2007, **72**, 1697–1706; (*c*) G. L. Levit, V. P. Krasnov, A. M. Demin, M. I. Kodess, L. Sh. Sadretdinova, T. V. Matveeva, V. A. Ol'shevskaya, V. N. Kalinin, O. N. Chupakhin and V. N. Charushin, *Mendeleev Commun.*, 2004, **14**, 293–295; (*d*) V. P. Krasnov, A. M. Demin, G. L. Levit, A. N. Grishakov, L. Sh. Sadretdinova, V. A. Ol`shevskaya, V. N. Kalinin and V. N. Charushin, *Russ. Chem. Bull.*, 2008, **57**, 2535–2539; (*e*) V. P. Krasnov, G. L. Levit, V. N. Charushin, A. N. Grishakov, M. I. Kodess, V. N. Kalinin, V. A. Ol'shevskaya and O. N. Chupakhin, *Tetrahedron: Asymmetry*, 2002, **13**, 1833–1835.

27 P. Morel, P. Schaffer and J. F. Valliant, *J. Organomet. Chem.*, 2003, **668**, 25–30.

28 (*a*) D. Zhao and Z. Xie, *Angew. Chem., Int. Ed.*, 2016, **55**, 3166–3170; (*b*) D. Zhao, J. Zhang and Z. Xie, *Angew. Chem., Int. Ed.*, 2014, **53**, 8488–8491.

29 T. P. Brauna, P. A. Gutsch and H. Zimmer, *Z. Naturforsch.*, 1999, **54b**, 858–862.

30 A. Buchard, B. Komly, A. Auffrant, X. F. Le Goff and P. A. Le Floch, *Organometallics*, 2008, **27**, 4380–4385.

31 L. Boubekeur, L. Ricard, N. Mezailles and P. Le Floch, *Organometallics*, 2005, **24**, 1065–1074.

32 P. Molina, A. Arques, A. Garcia and M. C. Ramirez de Arellano, *Tetrahedron Lett.*, 1997, **38**, 7613–7616.

33 P. Molina, A. Arques, A. Garcia and M. C. Ramirez de Arellano, *Eur. J. Inorg. Chem.*, 1998, 1359–1368.

34 R. S. Pandurangi, K. V. Katti, L. Stillwell and C. L. Barnes, *J. Am. Chem. Soc.*, 1998, **120**, 11364–11373.

35 (*a*) K. V. Katti, B. D. Santarsiero, A. A. Pinkerton and R. G. Cavell, *Inorg. Chem.*, 1993, **32**, 5919–5925; (*b*) J. Li, R. McDonald and R. G. Cavell, *Organometallics*, 1996, **15**, 1033–1041.

36 (*a*) Y. Sevryugina, R. L. Julius and M. F. Hawthorne, *Inorg. Chem.*, 2010, **49**, 10627–10634; (*b*) R. Cheng, Z. Qiu and Z. Xie, *Nat. Commun.*, 2017, **8**, 14827–14833; (*c*) R. M. Dziedzic, L. M. A. Saleh, J. C. Axtell, J. L. Martin, S. L. Stevens, A. Timothy Royappa, A. L. Rheingold and A. M. Spokoyny, *J. Am. Chem. Soc.*, 2016, **138**, 9081–9084.

37 G. K. Anderson and M. Lin, *Inorg. Synth.*, 1990, **28**, 60–63.

38 (*a*) E. W. Abel and S. A. Mucklejohn, *Phosphorus Sulfur Relat. Elem.*, 1981, **9**, 235–266; (*b*) R. Bielsa, A. Larrea, R. Navarro, T. Soler and E. P. Urriolabeitia, *Eur. J. Inorg. Chem.*, 2005, 1724–1736; (*c*) C. J. Wallis, I. L. Kraft, J. N. Murphy, B. O. Patrick and P. Mhrkhodavandi, *Organometallics*, 2009, **28**, 3889–3895; (*d*) S. D. J. Brown, W. Henderson, K. J. Kilpin and B. K. Nicholson, *Inorg. Chim. Acta*, 2007, **360**, 1310–1315.

39 S. J. Coles, P. Faulds, M. B. Hursthouse, G. C. Ranger, A. J. Toner and N. M. Walker, *J. Organomet. Chem.*, 1999, **586**, 234–240.

40 (*a*) R. Meijboom, A. Muller and A. Roodt, *Acta Crystallogr., Sect. E: Struct. Rep. Online*, 2006, **62**, m897–m899; (*b*) V. A. Stepanova, L. M. Egan, L. Stahl and I. P. Smoliakova, *J. Organomet. Chem.*, 2011, **696**, 3162–3168.

41 M. Alajarín, C. López-Leonardo and P. Llamas-Lorente, *Tetrahedron Lett.*, 2001, **42**, 605–607.

42 (*a*) M. Alajarín, C. López-Leonardo, P. Llamas-Lorente, D. Bautista and P. G. Jones, *Dalton Trans.*, 2003, 426–434.

43 L. A. Boyd, W. Clegg, R. C. B. Copley, M. G. Davidson, M. A. Fox, T. G. Hibbert, J. A. K. Howard, A. McKinnon, R. J. Peace and K. Wade, *Dalton Trans.*, 2004, 2786–2799.

44 (*a*) K. V. Katti, R. J. Batchelor, F. W. B. Einstein and R. G. Cavell, *Inorg. Chem.*, 1990, **29**, 808–814; (*b*) V. Cadierno, J. Diez, J. Garcia-Alvarez, J. Gimeno, N. Nebra and J. Rubio-Garcia, *Dalton Trans.*, 2006, 5593–5604.

45 (*a*) C.-Y. Liu, D.-Y. Chen, M.-C. Cheng, S.-M. Peng and S.-T. Liu, *Organometallics*, 1995, **14**, 1983–1991; (*b*) A. Arques, P. Molina, D. Aunon, M. J. Vilaplana, M. D. Velaso, F. Martinez, D. Bautista and F. J. Lahoz, *J. Organomet. Chem.*, 2000, **598**, 329–338; (*c*) L. Boubekeur, L. Ricard, N. Meezailles, M. Demange, A. Auffrant and P. Le Floch, *Organometallics*, 2006, **25**, 3091–3094.

46 (*a*) J. Vicente, A. Arcas, D. Bautista and M. C. R. de Arellano, *Organometallics*, 1998, **17**, 4544–4550; (*b*) T. Cheisson and A. Auffrant, *Dalton Trans.*, 2016, **45**, 2069–2078.

47 D. Bézier, O. Daugulis and M. Brookhart, *Organometallics*, 2017, **36**, 2947–2951.

48 M. G. Davidson, T. G. Hibbert, J. A. K. Howard, A. Mackinnon and K. Wade, *Chem. Commun.*, 1996, **19**, 2285–2286.

49 (*a*) S. C. To and F. Y. Kwong, *Chem. Commun.*, 2011, **47**, 5079–5081; (*b*) J. O. Yu, E. Lam, J. L. Sereda, N. C. Rampersad, A. J. Lough, C. S. Browning and D. H. Farrar, *Organometallics*, 2005, **24**, 37–47; (*c*) G. R. Newkome, D. W. Evans and F. R. Fronczek, *Inorg. Chem.*, 1987, **26**, 3500–3506; (*d*) N. M. Vinogradova, I. L. Odinets, K. A. Lyssenko, M. P. Pasechnik, P. V. Petrovskii and T. A. Mastryukova, *Mendeleev Commun.*, 2001, **11**, 219–220; (*e*) J. Autio, S. Vuoti, M. Haukka and J. Pursiainen, *Inorg. Chim. Acta*, 2008, **361**, 1372–1380.

50 F. Teixidor, G. Barbera, A. Vaca, R. Kivekäs, R. Sillampää, J. Oliva and C. Viñas, *J. Am. Chem. Soc.*, 2005, **127**, 10158–10159.

51 R. F. W. Bader, *Atoms in Molecules: A Quantum Theory*, Oxford, University Press, Oxford, 1990.

52 T. Lu and F. Chen, *J. Phys. Chem. A*, 2013, **117**, 3100–3108.

53 S. Boonseng, G. W. Roffe, J. Spencer and H. Cox, *Dalton Trans.*, 2015, **44**, 7570–7577.

54 P. K. Sajith and C. H. Suresh, *Inorg. Chem.*, 2011, **50**, 8085–8093.

55 F. Nanteuil and J. Waser, *Angew. Chem., Int. Ed.*, 2011, **50**, 12075–12079.

56 G. M. Sheldrick, *SADABS: Program for absorption correction using area detector data*, University of Göttingen, Germany, 1996.

57 G. M. Sheldrick, *Acta Crystallogr., Sect. A: Fundam. Crystallogr.*, 2008, **64**, 112–122.

58 L. Farrugia, *J. Appl. Crystallogr.*, 1997, **30**, 565.

59 J. M. Tao, J. P. Perdew, V. N. Staroverov and G. E. Scuseria, *Phys. Rev. Lett.*, 2003, **91**, 146401–146404.

60 K. A. Peterson, D. Figgen, M. Dolg and H. J. Stoll, *Chem. Phys.*, 2007, **126**, 124101–124112.

61 (*a*) M. Orbach, S. Shankar, O. V. Zenkina, P. Milko, Y. Diskin-Posner and E. van der Boom, *Organometallics*, 2015, **34**, 1098–1106; (*b*) J. Turek, I. Panov, M. Semler, P. Stepnicka, F. De Proft, Z. Padelkova and A. Ruzicka, *Organometallics*, 2014, **33**, 3108–3118.

62 T. Lu and F. Chen, *J. Comput. Chem.*, 2012, **33**, 580–592.

[i] Electronic supplementary information (ESI) available: Crystallographic data for all crystal structures, NMR spectra and optimized Cartesian coordinates obtained with DFT calculations. CCDC 1855597–1855602. For ESI and crystallographic data in CIF or other electronic format see DOI: 10.1039/c8dt04006k.